5-2022

MECHANISTIC INSIGHTS ON THE ROLE OF AMBRISENTAN, AN ENDOTHELIN TYPE-A RECEPTOR ANTAGONIST, IN BREAST CANCER

Ruba Saleem Lutfi Amer

United Arab Emirates University

College of Medicine and Health Sciences

Department of Microbiology and Immunology

MECHANISTIC INSIGHTS ON THE ROLE OF AMBRISENTAN, AN ENDOTHELIN TYPE-A RECEPTOR ANTAGONIST, IN BREAST CANCER

Ruba Saleem Lutfi Amer

This thesis is submitted in partial fulfilment of the requirements for the degree of Master of Medical Sciences (Microbiology and Immunology)

Under the Supervision of Prof. Basel al-Ramadi

May 2021

Declaration of Original Work

I, Ruba Saleem Lutfi Amer, the undersigned, a graduate student at the United Arab Emirates University (UAEU), and the author of this thesis entitled "*Mechanistic Insights on the Role of Ambrisentan, An Endothelin Type-A Receptor Antagonist, in Breast Cancer*", hereby, solemnly declare that this thesis is an original research work that has been done and prepared by me under the supervision of Professor Basel al-Ramadi, in the College of Medicine and Health Sciences at UAEU. This work has not previously formed the basis for the award of any academic degree, diploma or a similar title at this or any other university. Any materials borrowed from other sources (whether published or unpublished) and relied upon or included in my thesis have been properly cited and acknowledged in accordance with appropriate academic conventions. I further declare that there is no potential conflict of interest with respect to the research, data collection, authorship, presentation and/or publication of this thesis.

Student's Signature: _____   Date: _8 May 2021___

Advisory Committee

1) Advisor: Basel al-Ramadi

Title: Professor

Department of Microbiology and Immunology

College of Medicine and Health Sciences

2) Member: Maria J. Fernandez-Cabezudo

Title: Associate Professor

Department of Biochemistry

College of Medicine and Health Sciences

3) Member: Samir Attoub

Title: Professor

Department of Pharmacology

College of Medicine and Health Sciences

Approval of the Master Thesis

This Master Thesis is approved by the following Examining Committee Members:

1) Advisor (Committee Chair): Basel Al Ramadi

   Title: Professor

   Department of Microbiology and Immunology

   College of Medicine and Health Sciences

   Signature   Date 8 May 2021

2) Member: Maria J. Fernandez-Cabezudo

   Title: Associate Professor

   Department of Biochemistry

   College of Medicine and Health Sciences

   Signature   Date 9 May 2021

3) Member: Samir Attoub

   Title: Professor

   Department of Pharmacology

   College of Medicine and Health Sciences

   Signature   Date 9 May 2021

4) Member (External Examiner): Laura Rosanò

   Title: Professor

   Department of Biology and Biotechnology

   Institution: Institute of Molecular Biology and Pathology (IBPM)

   National Research Council (CNR), Italy

   Signature   Date 10 May 2021

This Master Thesis is accepted by:

Acting Dean of the College of Medicine and Health Sciences: Professor Jumaa Alkaabi

Signature _____ Date _____18/08/2021_____

Dean of the College of the Graduate Studies: Professor Ali Al Marzouqi

Signature _____ Date _____18/08/2021_____

Copy _____ of _____

Abstract

The activation of the endothelin receptor type A (ETAR) by its ligand endothelin-1 (ET-1) is well known for its role in vasoconstriction. Interestingly, ET-1 and ETAR are over-expressed in various human tumors, including breast cancer. Several studies described an important role for ETAR in cancer progression and metastasis. The extensive network of interactions that exist between ET-1 axis and other signaling pathways can trigger an autocrine and paracrine signaling that modulates different tumorigenesis processes, such as cellular proliferation and survival, epithelial-to-mesenchymal transition (EMT) and chemoresistance. The main objective of this study was to investigate the antitumor effects of Ambrisentan, a selective antagonist of ETAR, and FDA-approved for the treatment of pulmonary arterial hypertension (PAH), on tumor growth and metastasis using a syngeneic, orthotopic triple negative breast cancer (4T1) animal model. The results show a significant reduction in tumor growth and enhancement in overall animal survival in Ambrisentan-treated mice. This correlated with a significant decrease in the extent of tumor metastasis to the liver and lungs. Experiments using luciferase-expressing 4T1 tumor cells (4T1-Luc2) and in vivo life imaging (IVIS) of animals revealed a 5- and 18-fold decrease in the bioluminescence signal collected from the primary tumor site and distant organs, respectively, in Ambrisentan-treated mice. Using multi-color flowcytometry, accumulation of CD11b+Ly6G+ granulocytes in blood, peripheral lymphoid organs and lungs, a process driven by chemokines secreted by 4T1 cells, was inhibited by >50% following Ambrisentan treatment. Importantly, this was further confirmed by demonstrating >90% reduction in the number of 4T1-Luc2 tumor cells metastasizing to the lungs. Moreover, histological staining of liver tissue revealed a 43% decrease in the number of tumor foci in Ambrisentan treated group compared to control group. In an independent series of experiments, the effect of Ambrisentan on 4T1 cell growth was tested in the Chorioallantoic membrane (CAM) assay. The findings highlighted the capacity of Ambrisentan to inhibit tumor growth by ~25% independent of any effect on anti-tumor immune responses. To uncover the underlying mechanism for the anti-metastatic effect of Ambrisentan, the extent of angiogenesis was within the tumor tissue by immunohistochemical staining using CD31-specific mAb. The findings

revealed that total tumor vascularity was reduced by ~50%, mainly due to a decrease in the size of blood vessels in animals treated with Ambrisentan. Analysis of gene expression in 4T1 cells treated with Ambrisentan revealed significant inhibition (40-50%) of CXCL1 and MMP9, which are essential factors for tumor progression and metastasis. Taken together, this study provides a rationale for using Ambrisentan as a potential adjuvant in cancer therapy.

Keywords: Endothelin type A receptor (ETAR), Endothelin-1 (ET-1), Cancer metastasis, Ambrisentan, IVIS, Myeloid cells, Lungs, Granulocytes, CAM, Angiogenesis, CXCL1, MMP9.

Title and Abstract (in Arabic)

حول آلية عمل دواء الأمبريسينتان و الذي يعمل كمضاد لمستقبلات الإندوثيلين من النوع أ في سرطان الثدي

الملخص

يعرف تنشيط مستقبلات الإندوثيلين أ (ETAR) لدوره في تضييق الأوعية الدموية. و من المثير للاهتمام الإفراط في التعبير عن الإندوثيلين1 (ET-1) و مستقبلات اللإندوثيلين 1 في العديد من الأورام البشرية، مثل سرطان الثدي. كما وصفت العديد من الدراسات الدور الأساسي لمستقبلات الإندوثيلين أ في تطور الورم و انتشاره. يمكن أن تؤدي شبكة التفاعلات الواسعة القائمة ما بين محور الإندوثيلين و مسارات نقل الإشارات الأخرى على تنشيط إشارات autocrine و paracrine و التي يمكنها من التحكم في العديد من عمليات تكوين الأورام، مثل نمو و تكاثر الخلايا السرطانية و مقاومتها للعلاج الكيميائي و التي تساعد على انتشار الورم. تهدف هذه الدراسة للتحقق من التأثير المضاد للورم للأمبريسنتان، و هو مضاد انتقائي لمستقبلات الإندوثيلين من النوع أ، ومعتمد من قِبل هيئة الدواء و الأغذية الأمريكية (FDA) لعلاج ارتفاع ضغط الدم الشرياني الرئوي (PAH)، على نمو الورم و انتشاره في تجربة غير سريرية باستخدام النموذج الحيواني لسرطان الثدي السالب للمستقبلات الهرمونية الثلاث (4T1). أظهرت النتائج انخفاضًا ملحوظا في نمو الورم وتحسين في بقاء الحيوانات على قيد الحياة بشكل عام في الفئران المعالجة بالأمبريسنتان. وارتبط هذا أيضًا بانخفاض كبير في مدى انتشار الورم في الكبد والرئتين. من خلال استخدام خلايا السرطانية المعبرة عن اللوسيفراز (4T1-Luc) تم متابعة نمو الورم عن طريق استخدام التصوير في الجسم الحي (IVIS)، أظهرت البيانات التي تم جمعها انخفاضًا بمقدار 5 و 18 ضعفا في إشارة التلألؤ الحيوي المنبعثة من موضع الورم الرئيسي بالإضافة إلى الصادرة من الأعضاء البعيدة على التوالي في الفئران المعالجة. و باستخدام تحليل التدفق الخلوي (Flow cytometry) وجد انخفاضا في تجمع الخلايا الحبيبية المتعادلة (CD11b + Ly6G+ Granulocytes) في الدم و الأعضاء الليمفاوية و في الرئتين و هي عملية تتحكم بها الكيموكينات التي تفرزها خلايا (4T1), بنسبة أكبر من 50% كنتيجة للعلاج بالأمبريسنتان. علاوة، تم تأكيد ذلك من خلال إظهار انخفاض بمقدار 90% فأكثر في عدد خلايا ورم (4T1-Luc) المنتشرة في الرئة. بالإضافة إلى ذلك، أظهر التصبيغ النسيجي انخفاضًا في عدد بؤر الورم في أنسجة الكبد بنسبة 43% تقريبا في المجموعة

المعالجة بالأمبريسنتان. و في سلسلة مستقلة من التجارب، تم اختبار تأثير الأمبريسنتان على نمو خلايا 4T1 في الغشاء المشيمي-السقاء (CAM). و قد أبرزت النتائج قدرة الأمبريسينتان على تثبيط نمو الورم بنسبة 25% تقريبا، بعيدا عن أي استجابات مناعية ضد الورم. للكشف عن الآلية التي يعمل بها الأمبريسنتان كمضاد لانتشار الورم، تم دراسة مدى قدرة الورم على تكوين أوعية .

مفاهيم البحث الرئيسية: مستقبل الإندوثيلين من النوع أ، الإندوثيلين، ورم خبيث، أمبريسنتان، تصوير الجسم الحي، الخلايا النخاعية، الرئتين، الخلايا الحبيبية المتعادلة، الغشاء المشيمي-السقاء، أوعية دموية ورمية، CXCL1، MMP9.

Acknowledgements

Dedication

To my father (may Allah have mercy on him), my biggest supporter and my number one fan

Table of Contents

List of Tables

List of Figures

List of Abbreviations

ABT-627	Atrasentan
CAM	Chorioallantoic Membrane
CAM	Chorioallantoic Membrane
CCL2	C-C Motif Ligand 2
CCL5	Chemokine Ligand 5
CRC-SC	Colorectal Cancer- Stem Cell
CX3CL1	(C-X3-C Motif) Ligand 1
CX3CR1	Chemokine (C-X3-C Motif) Receptor 1
CXCL12	Chemokine Ligand 12
CXCR4	Chemokine Receptor 4
DAG	Diacylglycerol
DCs	Dendritic Cells
dH_2O	Distilled Water
E9	Embryonic Day 9
ECE1	Endothelin Converting Enzyme 1
ECM	Extracellular Matrix
EGF	Epidermal Growth Factor
EMA	European Medicines Agency
EMT	Epithelial-To-Mesenchymal Transition
ER	Estrogen
ERAs	Endothelin Receptor Antagonists
ET-1	Endothelin-1
ET-2	Endothelin-2
ET-3	Endothelin-3
ETAR	Endothelin Type-A Receptor
ETBR	Endothelin Type-B Receptor

FasL	Fas Ligand
FDA	Food And Drug Administration
GBM	Glioblastoma
GDP	Guanosine Diphosphate
gMDSCs	Granulocytic Myeloid Derived Suppressor Cells
GTP	Guanosine Triphosphate
GPCR	G Protein-Coupled Receptors
HER2	Human Epidermal Growth Factor 2
HPF	High Power Fields
IACUC	Institutional Animal Care and Use Committee
ICAM1	Intercellular Adhesion Molecule 1
IL-12	Interleukin-12
IL-6	Interleukin-6
ILK	Integrin-Linked Kinase
IP3	Inositol 1,4,5 Triphosphate
IVIS	*In Vivo* Imaging System
KC	Keratinocytes-Derived Chemokine
MAPK	Mitogen-Activated Protein Kinase
MCP1	Monocyte Chemoattractant Protein 1
MDSCs	Myeloid Derived Suppressor Cells
mMDSCs	Monocytic Myeloid Derived Suppressor Cells
MMP9	Matrix Metallopeptidase 9
MMPs	MAtrix Metallopeptidases
PAH	Pulmonary Arterial Hypertension
PAP	Pulmonary Artery Pressure
PBS	Phosphate Buffer Saline
PDGF	Platelet-Derived Growth Factor
PI3K	Phosphoinositide3-Kinases

PI-PLC	Phosphatidyl Inositol Specific Phospholipase C
PKA	Protein Kinase A
PKC	Protein Kinase C
PLC	Phospholipase C
PPETs	Pre-Pro-Endothelin
PR	Progesterone
PTK	Tyrosine Kinases
PVR	Pulmonary Vascular Resistance
RAP	Right Atrial Pressure
RBC	Red Blood Cells
TAM	Tumor-Associated Macrophages
TGF-β	Transforming Growth Factor-Beta
Th1	Helper T-Cell
Th2	Helper T-Cell
TNBC	Triple Negative Breast Cancer
TNF	Tumor Necrosis Factor
VEGF	Vascular Endothelial Growth Factor
WHO	World Health Organization
ZD4054	Zibotentan

Chapter 1: Introduction

1.1 Endothelin axis

1.1.1 Discovery of the endothelin receptors

In 1988, Yanagisawa and colleagues were the first to describe endothelin-1 (ET-1). They purified and sequenced an endothelial cell-derived peptide after observing an endothelium-independent contraction of isolated porcine coronary arteries (Yanagisawa et al., 1988). ET-1 is a small peptide of 21 aa (amino acid) residues, characterized by a single α helix, two essential disulfide bridges, Cys3-Cys11 and Cys1-Cys15, and six conserved amino acid residues at the C-terminus. Since its discovery, ET-1 has been found to be expressed in the genome of several species, including humans. However, human genome encodes two other endothelin isotypes, endothelin-2 (ET-2) and endothelin-3 (ET-3). The different endothelin isopeptides are highly homologous with conserved sequences; all are 21 aa polypeptides, containing two intrachain disulfide bonds, and an identical hydrophobic C-terminal hexapeptide (Ohlstein et al., 1996). Changes in the amino acid sequence between the different ET isoform is highlighted in Figure 1.

1.1.2 Endothelin biosynthesis

ET-1 is not a ready-made protein that is kept stored in endothelial cells. Instead, the production of ET-1 is regulated at the transcriptional level in response to various stimulants and inhibitors, thus allowing for massive changes in the amounts released. The ET-1 cDNA contains one single copy gene that encodes a long precursor polypeptide of 212 aa known as preproendothelin (PPETs). The human ET-1, ET-2,
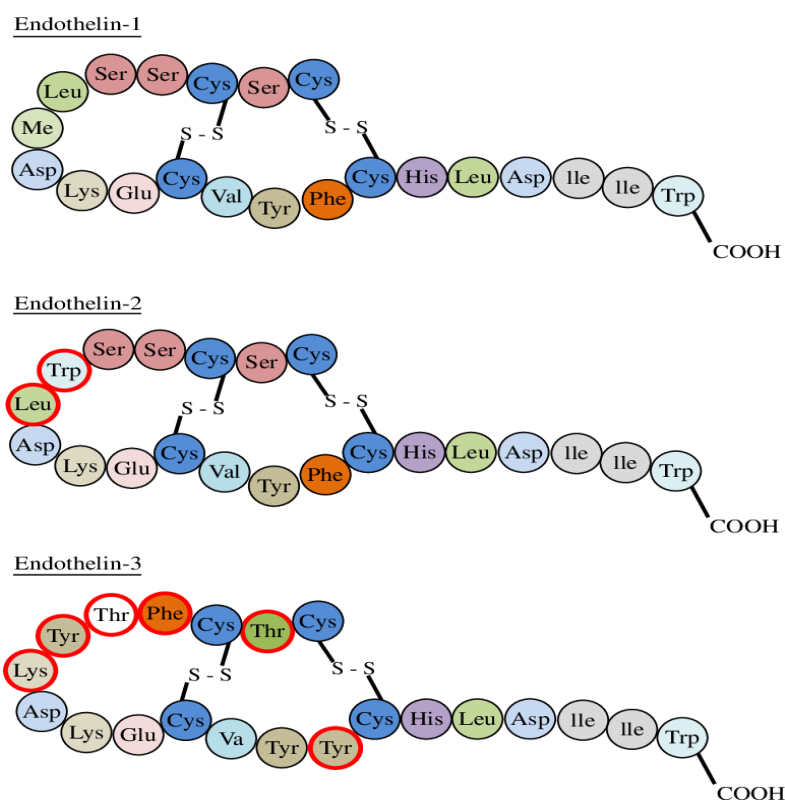
Figure 1: Amino-acid sequences of endothelin isoforms. The change in the amino acids sequence in the different isoforms compared to ET-1 is circled in red (Chester & Yacoub, 2014)

and ET-3 are separate gene products and have been located on chromosomes 6p23-23, lp34, and 20q13.2-13.3, respectively (Bloch et al., 1989). The EDN1 gene, which encodes for ET-1, is located on chromosome 6, containing five exons and spanning 6.8 kb (Rosanò et al., 2013). Preproendothelin will be further cleaved proteolytically by peptidase to form pro-ET-1, which is then activated and converted to 38 aa-long pro-ETs, known as big-ET1 by the activity of a subtilisin-like convertase/furin-like protease. Endothelin converting enzyme 1 (ECE1), or, alternatively, a chymase enzyme 6 then subsequently cleaves Trp21-Va122 of big ET-1 to release the mature form of the 21-aa- ET-1 peptide (Xu et al., 1994) (Figure 2). Following ET processing, peptides can either be secreted constitutively or it can be kept stored intracellularly in

granules and secreted in response to a pathway activation by a stimulus it can be secreted (Russell et al., 1998).
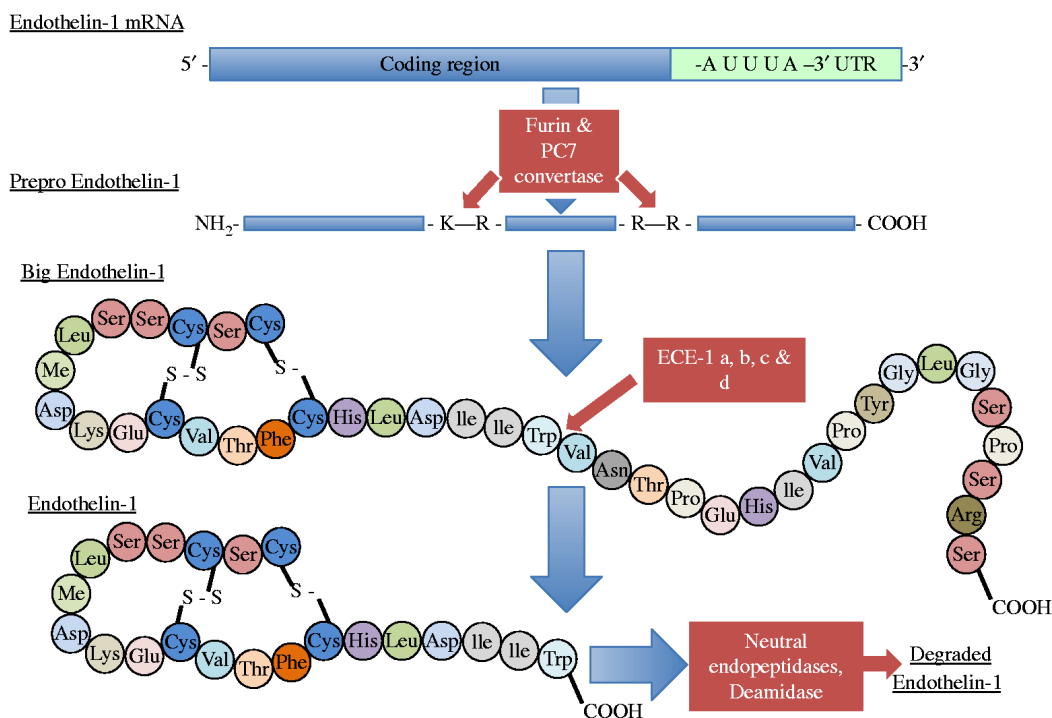
Figure 2: ET1 biosynthesis. EDN1 gene encode for 212 aa long precursor known as prepro-Endothelin. PPET is proteolytically cleaved and converted to the bigendothelin (38 aa long). Which will be subsequently cleaved by endothelin converting enzyme to fore the active for ET-1 (Chester & Yacoub, 2014).

1.1.3 Endothelin receptors (ETRs)

After their activation and secretion, ETs act mainly on two distinct receptors belonging to the G protein-coupled receptors (GPCR), seven transmembrane spanning superfamily, Endothelin Type-A receptor (ETAR) and Endothelin Type-B receptor (ETBR). The two receptors differ in their binding affinity to the different ETs and in their different cellular distribution. It has been found that ETAR binds ET-1 and 2 with the greatest affinity, (Kd = ~20-60 pM) compared to ET-3 (Kd = ~6500 pM), whereas

ET-1,2, and 3 all have the same affinity for ETBR (Kd = ~15 pM) (Rosanò & Bagnato, 2016). Several cells and tissues express endothelial axis components, such as smooth muscle cells, cardiac myocytes, mesangial cells, astrocytes and leukocytes. However, the main source of the endothelin axis components is the vascular endothelium. In humans, ETAR is found in the vasculature and is mainly expressed by the vascular smooth muscle cells, while ETBR is mainly expressed by smooth muscles cells and endothelial cells. In these cells, when ETs bind to ETAR, they induce vasoconstriction and proliferation, while their binding to ETBR induces vasodilation through the release of nitric oxide. In addition, ligand binding to ETBR can mediate vasoconstriction in certain vascular beds as well as bronchoconstriction in the respiratory tract (Aubert & Jeanneret, 2016).

1.2 ET Signaling pathway

1.2.1 G-Protein mediated GPCR signaling

As a GPCR, binding of ET to ETRs transduce the activation of signaling cascade through G proteins, which are named for their ability to bind Guanosine triphosphate (GTP) and Guanosine diphosphate (GDP). Heterotrimeric G proteins are consisting of 3 subunits, Gα, Gβ and G$_\gamma$ subunits (Tuteja, 2009). In their inactive form, Gα is bound to Gβγ dimer and GDP. On the other hand, the binding of agonist to the GPCR, result in receptor conformational change and trigger G proteins to exchange GDP for GTP on the Gα subunit leading to its activation and leads to the dissociation of Gβγ dimer from Gα. Following dissociation, each complex can interact with a variety effector system (Wang et al., 2018). G proteins are classified based on the α subunit into 4 main classes: Gαstimulatory (Gαs), Gαinhibitory (Gαi), Gαq, and

Gα12/13 (Tuteja, 2009). ETAR couples to Gαq and activates the PLC (phospholipase C) signaling (Gilman, 1984).

1.2.2 Cellular contraction

In the smooth muscles, binding of ET1 to ETAR induces the activation of phosphatidyl inositol specific phospholipase C (PI-PLC), this leads to the formation of inositol 1,4,5 triphosphate (IP3) and diacylglycerol (DAG). Increased IP3 then stimulates the release of stored Ca2+ from sarcoplasmic reticulum into the cytosol. The rapid elevation in intracellular Ca2+, in turn, causes smooth muscle contraction and then vasoconstriction (Khimji & Rockey, 2010). On the other hand, binding of ET-1 to ETBR on the endothelium induces the formation of nitric oxide (NO). In the absence of smooth muscle endothelin receptor stimulation, NO causes vasodilation. The cascade of ETAR-initiated events that lead to cellular contraction is shown in Figure 3.

1.2.3 Endothelin-1 Receptor/β-Arrestin-1 Axis

In response to ET binding, ET receptors can activate different signaling pathways in a G-protein independent manner, by forming complexes with β-arrestin (β-arr-1 or β-arr-2). β-arrestins, initially identified as negative regulators of GPCR-mediated signaling, are now recognized as scaffolds and adapters proteins (Lefkowitz & Shenoy, 2005). The binding of ET-1 to its receptors leads to the recruitment of β-arr1, which then shuttles into the nucleus where it forms a complex with histone acetyltransferase P300 (p300 HAT) involving different transcriptional factors and leading to the transcription of different target genes including ET-1. This will result in the amplification of the ET-1 autocrine loop (Maguire et al., 2012). In addition to its

nuclear function in ET-1 signaling, β-arr found to directly interact with multiple cytoskeletal components with various functions and localization (Shukla, Xiao, & Lefkowitz, 2011). It induces actin assembly activities and several upstream regulators which in turn lead to local invasion and metastasis (Semprucci et al., 2016). Thus, ETAR/β-arr1 signaling is a key role for cytoskeletal organization and Rho GTPase activity supporting cell motility (Rosanò & Bagnato, 2019; Tocci et al., 2016).

1.2.4 Crosstalk with other pathways

Endothelin signaling is extremely complex and activation of the ET axis can stimulate a number of various effector systems such as phospholipases D and A2, protein kinase A and C (PKA and PKC), as well as the protein tyrosine kinase and MAP-kinase (MAPK/ERK) pathways (Bremnes et al., 2000; Sasaki et al., 1998). ET-mediated activation of NF-κB, β-catenin, Hypoxia-inducible factor 1-alpha (HIF1-α) and Rho factor (ρ) has also been described (Nelson et al., 2003). Some of the pathways activated by ET-1 signaling lead to essential cellular responses that are illustrated in Figure 3. For example, tyrosine kinases (PTK), such as RAF and RAS, are stimulated by ET1 and promote the induction of RAF/MEK/Mitogen-activated protein kinase (MAPK) pathway, which in turn activates cell growth and metastasis.

1.3 Physiological role of endothelin

1.3.1 Receptors distribution

Since Endothelin is a potent, ubiquitous endothelium-derived vasoactive peptides, Endothelin receptors are expressed in all tissues, contributing to the maintenance of vascular tone. However, ETAR and ETBR are differentially expressed in the tissues. In humans, ETAR predominates on the smooth muscle of blood vessels,

while ETBR is the principal type in the kidney, localized in nonvascular tissues. In addition, epithelial cells and central nervous system glia and neurons also express ETRs.
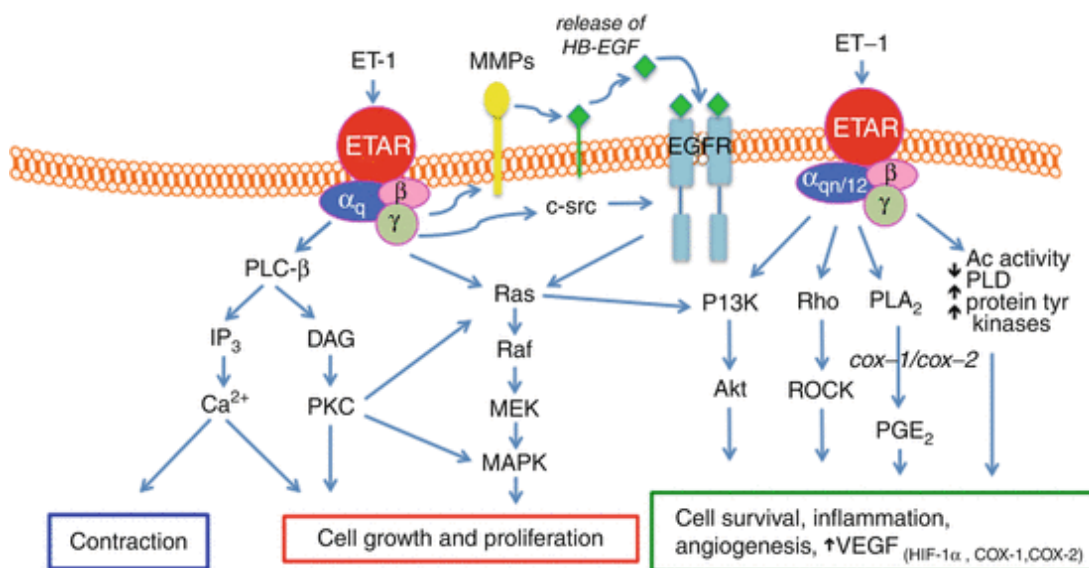
Figure 3: Endothelin pathway signaling. Activation of endothelin receptors stimulate the initiation of various downstream signaling cascades, which in turn induces several cellular responses (Dandan & Brunton, 2012).

1.3.2 Blood flow and vasoconstriction

Maintaining the blood flow in the body appears to be the most important physiological stimulus that regulates ET-1 synthesis and release. As a result of increase blood flow, ETBR acts as a "clearing receptor" to remove ET from the circulation. Its activation induces the release of endothelium-derived relaxing factors, such as nitric oxide (NO) and prostanoids which will cause vasodilation (Davenport, 2002). ET-1 mRNA is also upregulated by a variety of soluble factors including cytokines,

transforming growth factor-beta (TGF-β), tumor necrosis factor (TNF), interleukins, insulin, norepinephrine, angiotensin II and thrombin (Emori et al., 1992). It has also been shown that ET-1 mRNA is upregulated by hypocapnia and down regulated by hypoxia.

1.3.3 Other physiological function

In addition to its extremely important vasoconstrictor activity, endothelin can stimulate cellular proliferation, including smooth muscle cells (ETA) and astrocytes (ETB). In most of these cells, ET is thought to act as a co-mitogenic, enhancing the action of other growth factors such as platelet-derived growth factor (PDGF) (Kohno et al., 1994).

1.4 Endothelin axis expression in cancer

It has been found that both ETAR and ETBR are expressed by different cancer cells. However, the receptor expression profile differs in tumor cells when compared to normal tissues. Some cancers predominantly express ETAR such as ovarian, nasopharyngeal, thyroid, prostate, colon, pancreatic, gastric, renal, and breast cancers, while in other cancer cells ETBR is predominant, such as melanoma, glioblastoma multiforme (GBM), and astrocytoma. Moreover, the expression of the two receptors was reported in oral, lung, bladder, vulvar cancers, and Kaposi's sarcoma (Bagnato et al., 1995; Nelson et al., 2003; Nelson et al., 1995; Rosanò et al., 2013). In addition to that, overexpression of ET-1, ETAR and ETBR has been shown in various human tumors; ETAR overexpression was reported on breast cancer tissue in comparison with non-neoplastic tissue (Wülfing et al., 2005) and in prostate cancer, elevated expression of both ET-1 and ETAR was observed (Nelson et al., 2003). Studies have reported the

ability of ET to confer apoptosis resistance, stimulate new vessel formation, modulate immune responses and promote invasion and metastatic dissemination (Rosanò et al., 2013).

1.5 Endothelin receptor antagonists

Endothelin receptor antagonists (ERAs) are therapeutic alternatives to parenteral prostacyclin agents. They are currently classified as either ETAR-selective (ETAR/ETBR selectivity > 100) or dual ETAR/ETBR antagonists (equivalent selectivity to ETAR and ETBR). In contrast, very few ETBR-selective antagonists (ETAR/ETBR selectivity < 100) have been developed and evaluated in clinical trials to date. When given orally, ERAs competitively bind to ETAR and ETBR, causing a reduction in pulmonary artery pressure (PAP), pulmonary vascular resistance (PVR), and mean right atrial pressure (RAP). ETRs antagonist drugs are approved by the World Health Organization (WHO) for treatment of pulmonary arterial hypertension (PAH) in patients with class III or IV symptoms to improve exercise ability and decrease the rate of clinical deterioration (Galiè et al., 2016). There are currently three ET-receptor antagonists in clinical use, Bosentan, Ambrisentan and Macitentan, while drugs like Sitaxentan, which initially showed favorable results have been withdrawn from the market in 2010 due to issues relating to hepatic toxicity (Chester & Yacoub, 2014).

1.5.1 Bosentan

Bosentan, sold under the brand name Tracleer, is a dual ETAR/ETBR antagonist medication and was the first ERA to be used clinically. It has a higher affinity for ETAR compared to ETBR. It is available as film coated tablets for oral

administration and has a half-life of approximately 7 hours (Roux & Rubin, 2002). Treatment with Bosentan has been associated with elevations in serum aminotransferase levels during therapy and with rare instances of clinically apparent acute liver injury. It is metabolized by the CYP2C9 and 3A4 isoenzymes of cytochrome P450 and may therefore interact with drugs like cyclosporine A and birth control pills. Monthly monitoring of serum enzyme levels is recommended, with discontinuation when levels of the upper limit of the normal range (ULN) score above 8 times the ULN (2012).

1.5.2 Ambrisentan

Ambrisentan is approved by European Medicines Agency (EMA) and U.S Food and Drug administration (FDA) for the treatment of PAH. It is available under the brand name, Letairis and Volibris. It preferentially blocks ETAR as it has 4000 times greater affinity for ETAR compared to ETBR. Ambrisentan has a half -life of ~15 hours, making it suitable to be taken daily (Barst, 2007). Unlike other ERAs, Ambrisentan can get metabolized by glucuronidation and it does not interact with warfarin in the liver. Ambrisentan has advantages over other ETAR blockers, such as lower reported rates of liver toxicity (Newman et al., 2007).

1.5.3 Macitentan

Macitentan sold under the brand name Opsumit, is a dual ETAR/ETBR antagonist that was developed by modifying the structure of Bosentan to make sulphonamide derivatives. Macitentan has improved tissue penetration and high affinity for both receptors, hence a lower dose is required to achieve a similar effect of Bosentan. Macitentan has a half-life of approximately 6–8.5 and 14–18.5 hours

depending on the dose and it is slowly absorbed by the body. There was no effect of macitentan on bile salts indicating no toxic effect on hepatic function (Sidharta et al., 2013; Sidharta et al., 2011).

1.5.4 ERA and pregnancy

Studies have demonstrated the importance of ET1 axis signaling during early embryonic development. ET-1/ETAR signaling pathway was shown to be involved in early induction, migration and maintenance of neural crest specification (Bonano et al., 2008). Therefore, blocking of ETRs using ERAs drugs can affect normal embryo-fetal development. Mice carrying targeted homozygous mutations for the ET-A receptor or ET-1 died shortly after birth due to severe defects in the formation of neural crest derivatives (Clouthier et al., 1998; Kurihara et al., 1995; Pla & Larue, 2003). The three ERAs approved for the treatment PAH, Bosentan, Ambrisentan and Macitentan are listed in the Pregnancy Prevention Program (PPP) and are likely teratogenic (de Raaf et al., 2015; Enevoldsen et al., 2020).

1.6 Properties of tumors

Cancer happens when cells divide and grow abnormally resulting in a visible growth called tumor. Tumor cell have the ability to grow continuously, without being controlled by the main phases of the cell cycle. Some type of cancer has rapid cells growth, while others grow with a slower rate. Tumor cells can infiltrate and destroy normal body tissue and also have the ability to spread throughout the body. Cancerous cell is characterized by uncontrollable cell cycle, change in genomic information, rapid growth and increase cell mobility (Hanahan & Weinberg, 2011). Morphologically, malignant cells can be identified by the presence of a large nucleus, abnormal mitotic

figures, high nuclear cytoplasmic ratio, irregular contour, and a scarce cytoplasm intensely colored or, on the contrary, pale (Baba & Câtoi, 2007). Neoplastic cells function differently when compared to normal cells, these functional changes cause the formation or elimination of different active substances, including, growth factors, hormones, lytic enzymes. The secretion of lytic enzymes promotes cancerous cell mobility and dissemination. Tumors evolving from neoplastic cell composed of a highly heterogeneous cell population. This heterogeneity is continuously changing in time and can gradually change and increase tumor aggressiveness and acquire invasiveness and metastatic characteristics.

1.6.1 Regulation of tumor metastasis

Cancer cell metastasis is the process in which a tumor cell migrates from the primary tumor site and colonize a secondary site in distant organ. It is a complex process, and up to date the regulatory mechanism of tumor cell migration and invasion is not fully defined. However, for a tumor cell to successfully colonize a distant target organ, there are essential steps that it needs to go through. Failure to achieve any of those steps will result in metastasis inefficiency. As shown in Figure 4, first cells in the primary tumor need to detach and invade adjacent tissues and basement membrane. Then cells have to enter and survive in nearby blood vessels or lymphatic channels to be carried through the circulation to a distant organ. Eventually cells will arrest in small vessels within the distant organ, extravasate into the surrounding tissue and proliferate at the secondary site forming a secondary lesion (Hunter et al., 2008).
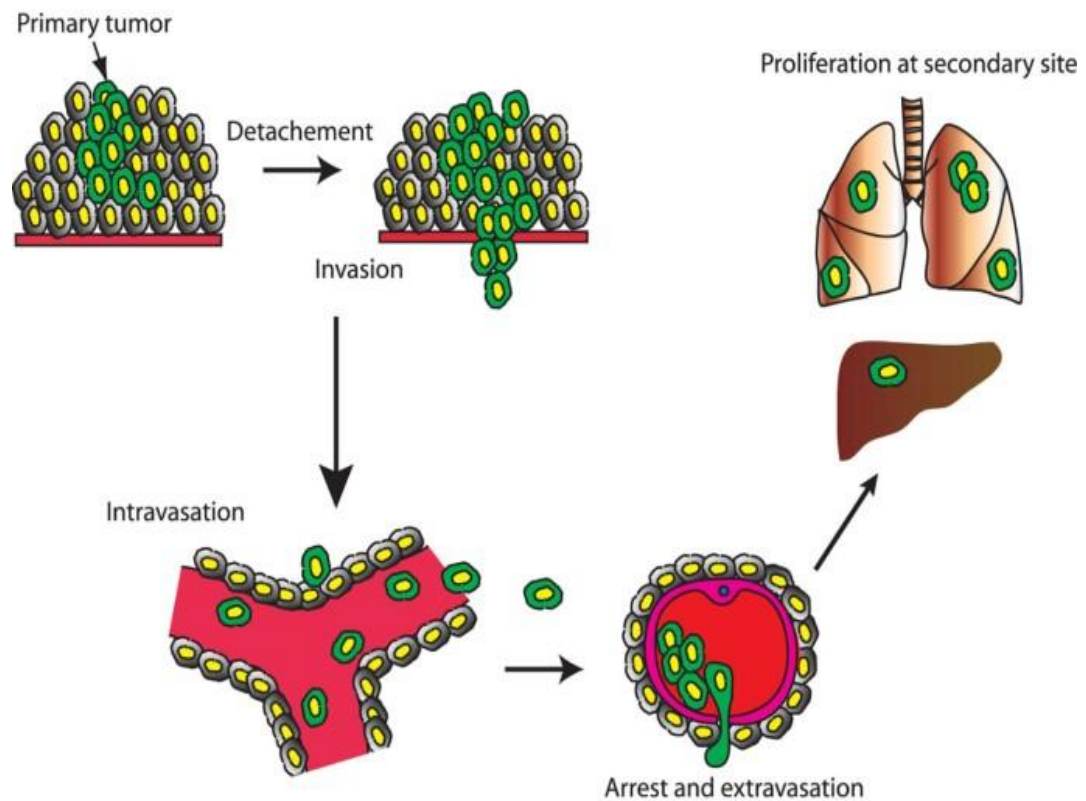
Figure 4: Tumor cells metastasis steps. cells from the primary tumor detach and invade the adjacent tissue, then to a blood vessels or lymphatic channels. Cells arrest and extravasate to distant target organ. There cells proliferate to form secondary lesion (Hunter et al., 2008).

1.6.1.1 Inflammatory chemokines and metastasis

Tumor growth and progression is promoted by multiple soluble factors secreted by both, tumor cells and stromal cells in the tumor microenvironment. This includes growth factors such as TGF and platelet-derived growth factor (PDGF) and cytokines such as chemokines. Chemokines are best known for their role in cells recruitment and movement according to a chemokine gradient. Cells expressing specific chemokine receptors will home toward the higher concentration of the ligand. During inflammation, chemokine induce specific recruitment of lymphocytes,

dendritic cells and macrophages. However, increasing evidence demonstrated the role of chemokines in tumor progression and metastasis (Allavena et al., 2011; Ben-Baruch, 2006). Inflammatory chemokines can control and regulate the homing and extravasation of tumor cells to distant organs. It has been reported that tumor cell derived chemokine (C-C motif) ligand 2 (CCL2), also referred to as monocyte chemoattractant protein 1 (MCP1), directly activates endothelial cells and with the help of monocytes, it facilitates tumor cell extravasation. Also, the recruitment of myeloid-derived suppressor cells (MDSC) to metastatic sites is induced by the inflammatory chemokines CCL2 and chemokine ligand 5 (CCL5) (Borsig et al., 2014). Those are immature myeloid cells with the ability to downregulate adaptive immunity and support tumor cells growth and progression. Furthermore, expression of Fractalkine also known as chemokine (C-X3-C motif) ligand 1 (CX3CL1) in the bone facilitates metastasis of tumor cells that express its receptor, chemokine (C-X3-C motif) receptor 1 (CX3CR1) to this site. In clinical studies, the effect of chemokines on tumor metastasis was first reported on breast cancer tissue. It has been found that in response to the expression of (CXC) chemokine ligand 12 (CXCL12) (CXC), cancer cells expressing chemokine receptor 4 (CXCR4) metastasize to the lymph nodes and lungs (Müller et al., 2001). CXCR4 is found to be expressed in the bone marrow and liver, CXCL12 is considered to be the sole ligand for CXCR4 (Kang et al., 2003; Wendel et al., 2012). In consequence, it has been found that breast cancer cells metastasize to the different organs in a CXCR4-dependent manner. High level of CCL2 and/or CCL5 was connected with poor outcome and shorter disease-free survival after surgery in patients with colon, breast, cervical and prostate cancer (Lu et al., 2006; Soria et al., 2008; Ueno et al., 2000; Velasco-Velázquez et al., 2012; Yoshidome et al., 2009; Zijlmans et al., 2006). High expression levels of CCL2 in

breast cancer tissue lead to an elevation in the tumor-associated macrophages (TAM) infiltration and increase in vessel density due to angiogenesis. In 4T1 cells, a murine breast cancer cells, elevated expression of CCL5 mediated spontaneous cells metastasis to lungs and liver (Stormes et al., 2005). CCL5 knockdown in 4T1 cells strongly reduced tumor cells metastasis that was linked with a reduced expression of MMP-10 and MMP-2. This finding highlights the role of CCL5 in facilitating 4T1 cells metastasis through modulation of matrix metalloproteinase production.

1.6.2 Tumors and the immune system

Tumor cells can suppress immunity by different ways, systemically and at the level of the tumor microenvironment. They can produce molecules such as soluble Fas ligand (FasL) and TGF-β, that work as immunosuppressor (Houston et al., 2003; Teicher, 2007). Moreover, through its progression, a growing tumor can recruit different components of the host response to its microenvironment. At first, tumor antigens attract dendritic cells (DCs), that take up the antigen and produce interleukin-12 (IL-12). In the draining lymphoid nodes, DCs stimulate the differentiation of type 1 helper T-cell (Th1). That will help to expand CD8 cytotoxic T-lymphocytes that can destroy tumor cells through the effector molecules granzyme B and perforin. However, another set of tumor antigens can promote maturation of a different type of dendritic cells, which produce the interleukin-6 (IL-6), proinflammatory cytokines and tumor necrosis factor α (TNF-α) and results in the activation of type 2 helper T-cell (Th2) that are not effective in tumor rejection. It has also been found that tumors recruit regulatory T cells, tumor associated macrophages (TAMs) and myeloid-derived suppressor cells (MDSC), all of which are known for their role to suppress antitumor effector T cells (Finn, 2008). High numbers of these cells were detected in ovarian

cancer and non–small-cell lung cancer (Woo et al., 2001). In addition, tumors can have a systemic immunosuppressive effect. In patients with head and neck cancer, an increase in regulatory T cells has been found in the peripheral blood (Bergmann et al., 2007; Chikamatsu et al., 2007). In colorectal cancer and pancreatic tumors there was an increase in numbers of activated granulocytes (Schmielau & Finn, 2001) and MDSCs (Nagaraj & Gabrilovich, 2007), both of which can suppress tumor specific T-cells in mice (Sinha et al., 2007).

1.6.2.1 Chemokines regulate Leukocytes recruitment to the metastatic site

Versican is a large proteoglycan found in the extracellular matrix and can recruit leukocytes by forming a chemokine gradient. Versican facilitates tumor metastasis to the lung through enhancement of tumor promoting inflammatory responses and releasing CCL2. Accordingly, the recruitment of monocytes and myeloid cells expressing chemokine receptor 1,2 and 5 (CCR1-, CCR2- and CCR5) was correlated to cancer progression (Lu & Kang, 2009; Qian et al., 2011; Robinson et al., 2003; Wolf et al., 2012; Zhao et al., 2013). In breast cancer cells expressing CCL5, tumor growth and progression was directly related to the infiltration of leukocytes expressing CCR1- and CCR5. The use of Met-CCL5 a CCR1 and CCR5 antagonist significantly retards tumor growth of already established tumors (Robinson et al., 2003). Moreover, the recruitment of CCR2- positive monocytes to the metastatic sites was identified as an essential factor for tumor metastasis in colon, breast, and lung cancer (Qian et al., 2011; Wolf et al., 2012).

1.7 Breast cancer

Breast cancer is considered as the most common malignancy in women worldwide. Approximate of 2.1 million women were newly diagnosed with breast cancer in 2018 only, and 626,679 women with breast cancer died (Bray et al., 2018). Early detection of cancer in the breast without spreading to other organs or only spread to the axillary lymph nodes can successfully be treated in 70-80% of patients. However, when breast cancer is metastatic at diagnosis, what known as advanced breast cancer is considered uncurable and treatment only prolongs survival and improve quality of life. At the molecular level, breast cancer is very heterogenous. It has been traditionally classified based on the presence or absence of the steroid hormones receptors, estrogen (ER) and progesterone (PR), and the epidermal growth factor receptor family member (HER2). Currently breast cancer is clinically classified into five subtypes based on the histological and molecular characteristic. The different breast cancer subtypes are illustrated on Figure 5.

1.7.1 Triple negative breast cancer

Triple negative breast cancer (TNBC) is a subtype of breast cancer that based on immunohistochemistry staining is negative for the three receptors: ER, PR and HER2. However, TNBCs are heterogeneous in their molecular characteristics, thus patients with TNBC have a wide variety of responses to chemotherapy (Medina et al., 2020). TNBC is known for its aggressive nature and the ability to metastasize to distinct organs, such as lung, liver and bone. TNBC account for 10-20% of invasive breast cancer cases (Aysola et al., 2013) and to date it lacks targeted therapies.
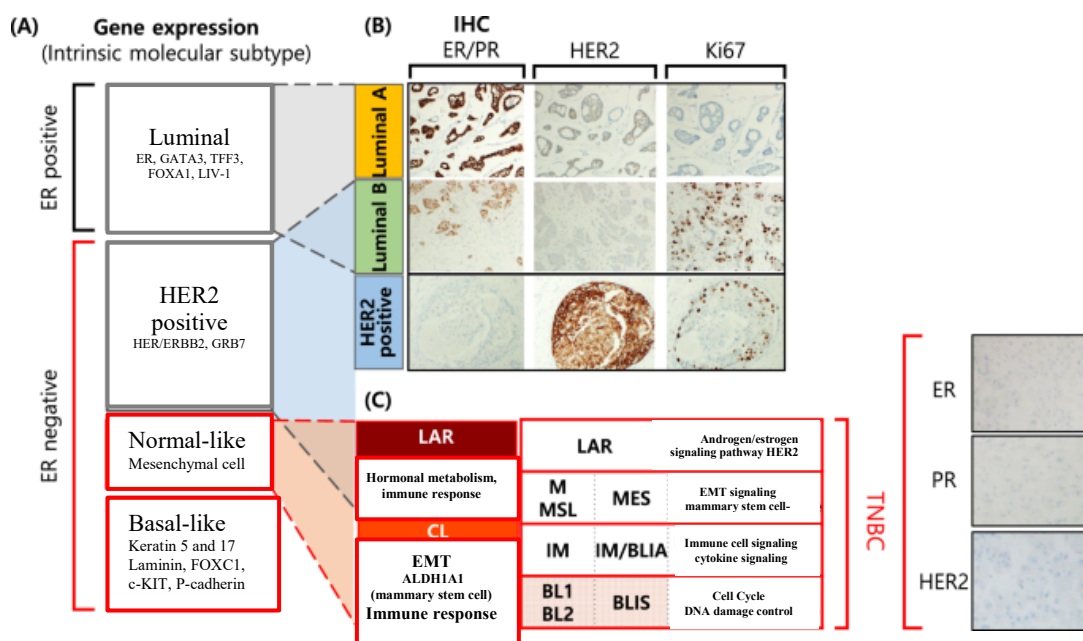
Figure 5: Schematic diagram of breast cancer classification by both gene expression and immunohistochemical staining. A. Intrinsic molecular subtypes of breast cancer based on gene expression, B. Immunohistochemical features of non-TNBC subclassification C. TNBC distinct subtypes according to gene expression patterns and significant molecular features of each subtype. TNBC shows negativity for ER, PR, and HER2. ER estrogen receptor, PR progesterone receptor, HER2 human epidermal growth factor receptor 2, IHC immunohistochemistry, LAR luminal androgen receptor, CL claudin low, M mesenchymal, MSL mesenchymal stem-like, IM immunomodulatory, BL basal-like, MES mesenchymal, BLIA basal-like immune-activated, BLIS basal-like immunosuppressed, EMT epithelial-mesenchymal transition, TNBC triple-negative breast cancer (Lee, Oh, Go, Han, & Choi, 2020)

1.7.1.1 Murine cellular model of triple negative breast cancer (4T1 cells)

4T1 is a murine cell line model for triple negative breast cancer, was first isolated by Fred Miller and his colleagues (Aslakson & Miller, 1992; Dexter et al., 1978). 4T1 tumor, transplanted in BALB/c mice is highly invasive and can spontaneously metastasize from the primary tumor in the mammary pad to different distant organs including blood, lungs, liver, lymph nodes, brain, and bone, making it a great model to study metastatic breast cancer. Kinetics analysis of the primary tumors

collected from 4T1-tumor bearing mice has shown that, orthotopic transplant of 4T1in the fat mammary pad causes splenomegaly and increases the hematopoietic cells infiltrate (CD45+) in the primary tumor site, mainly CD11b+ myeloid cells, with a F4⁄80+CD11c+ Gr-1+ phenotype (DuPre et al., 2007). Those are immature myeloid cells that are capable of differentiating into macrophages, dendritic cells, or granulocytes under the influence of certain cytokines or growth factors. On the other hand, analysis of the lung and liver, revealed the accumulation of granulocytes (Gr1+CD11b+ but F4/80-/CD11c-) myeloid phenotype population. It has been found that those neutrophils are gathered at the premetastatic site in the lung and produce leukotrienes which in turn will recruit highly tumorigenic breast cancer cells to the lung and thereby promote the seeding and colonization of tumor cells (Xie et al., 2017). In addition, it has been reported that 4T1 cells their selves produce neutrophils attractant chemokines such as, chemokine ligand 5 (CCL5) also known as RANTES, monocyte chemoattractant protein-1 (MCP-1/CCL2) and keratinocytes-derived chemokine (KC/CCL1). Which indicates that 4T1 cells and myeloid infiltrating cells are working in loop to induce tumor cells metastasis and colonization to the metastatic sites.

1.8 ET- axis and tumor growth

The autocrine ET-1 signaling in various tumor cells, functions as a mitogen and stimulate cancer cells proliferation. This signal can be amplified by interaction with different growth factors, including epidermal growth factor (EGF) and vascular endothelial growth factor (VEGF), basic fibroblast growth factor, insulin, insulin-like growth factor, PDGF, TGF-β and IL-6 (Nelson et al., 2003; Rosanò et al., 2013). Different studies using prostate, cervical, and ovarian cancer cells, showed that the

blockade of ET-1 receptor with receptors antagonists such as Zibotentan (ZD4054) and Atrasentan (ABT-627), lead to a significant growth inhibition and apoptosis induction. The combination of chemotherapeutic drugs with BQ123, Atrasentan, and Zibotentan, the selective ETAR antagonists or with dual ETAR and ETBR antagonist, Macitentan, improved the antitumor activity (Maffei et al., 2014; Nelson et al., 2003; Rosanò et al., 2014; Rosanò et al., 2013). Different tumor cells escape apoptosis by modulating well-known cell survival pathways, such as dependent protein kinase B (Akt), Phosphoinositide 3-kinases (PI3K), and NF-κB (Banerjee et al., 2007; Nelson et al., 2005). In prostate cancer cells, the use of Atrasentan, selective ETAR antagonist, inhibited the NF-κB DNA-binding activity, correlated with a decrease in the levels of the anti-apoptotic proteins Bcl-2, Bcl-xl and survivin, causing apoptotic cell death (Banerjee et al., 2007). Using ovarian cancer cells, it was found that ET-1 phosphorylated the anti-apoptotic protein Bcl, which lead to the inhibition of paclitaxel-induced apoptosis. Moreover, when the specific ETAR antagonist BQ123 was used, it restored the apoptotic response (Del Bufalo et al., 2002). In addition, numerous in vitro and in vivo experiments were performed on ovarian, prostate, colon and cervical cancer cells to study the effect of combining ET receptors antagonist and chemotherapy reagents, and all showed an improved induction of cell apoptosis (Bagnato et al., 2002; Banerjee et al., 2007; Del Bufalo et al., 2002; Kim et al., 2011; Kim et al., 2012; Nelson et al., 2005; Rosano et al., 2003).

1.9 ET1 role in tumor cell invasion and metastasis

A key feature distinguishing tumor cells from normal cells, is their capability to migrate and spread throughout the body by two related mechanisms, invasion and metastasis. During tumor progression, tumor cells regulate the synthesis and

production of the substances that bind cells to their surroundings, in addition to the release of proteases to lose cell-cell junctions allowing cancer cells to convert to more mesenchymal phenotype, facilitate invasion of extracellular matrix (ECM) and escape the primary tumor site (Polyak & Weinberg, 2009). In the aggressive model of triple-negative breast cancer (TNBC), it has been found a direct relation between lactoferrin and cells invasiveness, which was promoted through increasing ET1 expression and secretion (Ha et al., 2011). When BQ123 was added to the TNBC cells in culture, the ability of ET1 lactoferrin to promote cell migration was impaired.

1.9.1 MMPS and integrins

Increasing cell motility and migration depends on the ability of the cells to express different molecules and metastasis proteinases, among those are the soluble matrix metallopeptidases (MMPs) and integrins that facilitate the attachment of cells to the ECM, in addition to the modulation of cellular functions and behavior by delivering intracellular messages. ET1 activates varieties of soluble MMPs, including MMP2, MMP9, MMP3, MMP7 and MMP13. It also, increases the MMP/TIMP ratio by activating membrane type-1-MMP (MT1-MMP) and decreasing the release of tissue inhibitor of MMP1 (TIMP1) and TIMP2, which induces the rapid degradation of the ECM (Rosanò et al., 2001; Wu et al., 2012). In cultured glioblastoma (GBM) cells, exogenous ET-1 induced tumor cell migration that was correlated with an increase expression of MMP-9 and MMP-13 (Hsieh et al., 2014). Moreover, several studies on ovarian cancer and melanoma cells suggested the potential effect of ET1 on metastatic colonization by modulating β-integrins activation. The crosstalk between integrin-linked kinase (ILK), an intracellular serine/threonine kinase and ET1 promotes binding of ILK to the cytoplasmic domains of β1 integrin subunits,

connecting integrins to the actin cytoskeleton, controlling the spread of the cells and actin organization required for cell motility (Bagnato et al., 2004; Rosanò et al., 2006).

1.9.2 RHO-GDI2

Reduced expression of the GDP dissociation inhibitor (RhoGDI2), a metastasis suppressor, was found to decrease survival of patients with advanced lung metastatic bladder cancer. When DNA microarrays were performed to identify genes affected by RhoGDI2 reconstitution, ET1 suppression was observed (Titus et al., 2005). In the same model, treatment with Atrasentan and Zibotentan inhibited lung metastasis, suggesting the importance of ET1 in the bladder cancer microenvironment to promote pulmonary metastasis, thus identifying ET1 as a potential biomarker for lung metastasis (Said et al., 2011; Titus et al., 2005).

1.10 Effect of ET-1 on angiogenesis

Angiogenesis is the process of forming a network of blood vessels to support tumor growth and an important mechanism in tumor cells progression and metastasis. It is regulated by multiple conditions in the tumor microenvironment, including local hypoxia. It has been showed that ET1 works as mitogen for fibroblasts, vascular smooth muscle cells, blood and lymphatic endothelial cells (Nelson et al., 2003). Moreover, ET-1 found to stimulate angiogenesis process independently and through the induction of VEGF, expression of ET-1 and its receptor ETBR was increasing in correlation with VEGF and its receptors (VEGFR1 and VEGFR2) (Salani et al., 2000; Spinella et al., 2009; Wu et al., 2014).

1.11 ET-1 and immune cells

1.11.1 Inflammation and macrophages

ET1 can regulate differentiation and activation of tumor associated macrophages (TAMs). The expression of ETBR by macrophages allows them to travel towards ET1 secreted by different tumor cells. It has been reported that the secretion of ET1 by bladder cancer cells, triggers macrophages and induce pro-inflammatory cytokines and chemokines, such as IL-6, CCL2, COX2 and MMPs, which enable the primary cancer cells to migrate to the lungs. Interestingly, when ETAR antagonist, Zibotentan was used and macrophages were depleted, lung metastasis was suppressed (Said et al., 2011). In a breast cancer model, macrophages induced the expression of ET-1 and its receptor by the cancer cells, promoting the transendothelial migration of cancer cells (Chen et al., 2014).

1.11.2 Dendritic cells

Dendritic cells the most efficient antigen presenting cells were found to produce ET-1 and highly express ETAR and ETBR, especially during their maturation (Guruli et al., 2004). Interestingly, depending on which receptor is being activated, dendritic cells can respond differently. Blockade of ETAR using Atrasentan significantly reduced the expression of CD83, a dendritic cells maturation marker. It also reduced the production of IL-12, which impairs the ability of DC to stimulate T cells by dendritic cells and promoted cell apoptosis. On the other hand, blockade of ETBR by A192621 increased the expression of CD83 and improved dendritic cell survival.

1.11.3 Lymphocytes

ETBR overexpression was linked to the inhibition of T cells homing to the tumors. In ovarian cancer cells, ETBR signaling decreased tumor infiltrating lymphocytes and the use of ETBR antagonists abrogated this effect (Buckanovich et al., 2008; Kandalaft et al., 2009; Kandalaft et al., 2011). Moreover, it has been found that ETBR inhibits the expression of endothelial intercellular adhesion molecule 1 (ICAM1) preventing the adhesion of T cells to the endothelium.

1.12 ET-1 antagonists in clinical trials

The importance of ET1 signaling for tumor progressing and its role in promoting cancer cells metastasis and colonization, make it a rational target for cancer therapy. The promising preclinical results from cells and animal models on ET receptors antagonist therapy in cancer, opened the door to initiate different clinical trials. The dual ETAR and ETBR antagonists Bosentan and Macitentan and the specific ETAR antagonist Zibotentan, Atrasentan and YM-598, all have been evaluated in clinical settings. A phase III trials in patients with non-metastatic prostate cancer or advanced metastatic prostate cancer, Atrasentan and Zibotentan, each have been evaluated. ETRAs were giving either alone as a monotherapy or combined with docetaxel as combination therapy. All the trials, unfortunately, failed in patients with well-established tumor (Bagnato et al., 2011; Morris et al., 2005). In a phase I/II trial in patients with platinum-resistant recurrent ovarian cancer, Atrasentan was combined with doxorubicin. Limited number of patients showed a sign of prolonged survival (Witteveen et al., 2010). The reasons for this failure might be that ERA drugs have been used for patients with established metastatic disease suggesting that ERAs have

no effect on advanced tumors. Therefore, new therapeutic strategies need to explore the potential of Ambrisentan and other ERAs as adjuvant drug for patients with non-metastatic disease to prevent metastasis.

Chapter 2: Hypothesis

Endothelin axis is composed mainly of the ligand endothelin-1 (ET-1) and two main receptors, ETAR and ETBR. When ET-1 binds to its receptors, it stimulates the initiation of several signaling pathways that play a key role in multiple cellular processes such as, cell proliferation, migration, survival and apoptosis. Moreover, activation of endothelin receptors in particular the binding of ET1 to ETAR has been implicated in the development of several cancers. In some tumors, ET1 acted as a co-mitogen that induces cancer cells proliferation. Also, ET axis has shown to promote epithelial to mesenchymal transition and induce tumor cells migration and invasion. Relaying on the previous findings, this study hypothesizes that blocking ETAR signaling could retard tumor growth and metastasis and enhance host survival in the invasive triple negative breast cancer animal model.

Chapter 3: Aim and Objectives of the study

This study aims to investigate the in vivo effects of the selective ETAR antagonist Ambrisentan on metastatic breast cancer using a preclinical animal model. Ambrisentan is a selective ETAR antagonist approved by the U.S Food and Drug administration (FDA) and European Medicines Agency (EMA) for the treatment of PAH. Ambrisentan lower rate of liver toxicity possess advantages over other ETAR antagonists, however, the anti-tumor potential of Ambrisentan is yet to be investigated. Specific aims in this study are:

• Investigate the effect of Ambrisentan on tumor growth and metastasis as well as host survival in the preclinical 4T1 TNBC model

• Analyze the underlying mechanism for the action of Ambrisentan

Chapter 4: Materials and Methods

4.1 Materials

4.1.1 Mice

BALB/c mice were purchased from Jackson Laboratory (Bar Harbor, ME, USA), bred in the animal facility at the College of Medicine and Health Science, United Arab Emirates University (CMHS, UAEU). Mice were housed in plastic cages with a controlled light and dark cycle of 12 hours each at 24-26°C and received rodent chow and water ad libitum. All animals for this study were female and used at 8-12 weeks of age, weighing 18-22 g. All studies involving animals were carried out in accordance with, and after approval of the animal research ethics committee of the UAEU (Protocol no.AE/06/81).

4.1.2 Standard solutions

For the different techniques, different solutions were used. Table 1 shows the preparation of each solution.

Table 1: Standard solutions

Solution	Preparation
10x PBS	87.66 g NaCl, 2.56 g NaH2PO4.H_2O and 11.94 g Na2HPO4 dissolved in 1 L of distilled water.
Staining buffer for flow cytometric analysis	1 ml fetal calf serum and 0.1 g NaN3 was dissolved in 100 ml PBS.
Retrieval solution for immunocytochemistry	1.21 g Tris base, 0.37 g EDTA with 1000 ml water, pH adjusted to 9.
Blocking buffer (BSA) for immunocytochemistry	1 g albumin from bovine serum with 100 ml PBS with tween.
RBCs lysis buffer	8.3g ammonium chloride, 1g potassium bicarbonate and 1.8ml of 5%EDTA in 1L of distilled water and filtered through 0.2μm filter
10% Formalin for fixation	100 ml 37% formaldehyde in 900 ml PBS.

4.1.3 List of antibodies used for FACS staining

All antibodies used for flowcytometry experiments are shown in Table 2.

Table 2: List of antibodies used for FACS staining

Antibody	Host	Conjugate	Catalogue #	Company	Dilution (ug/ml)
CD16/CD32	Rat	-	101302	Biolegend	10
CD45	Rat	APC	103112	Biolegend	2.5
CD3	Rat	Brilliant Violet 785™	100232	Biolegend	2.5
CD3	Rat	FITC	100306	Biolegend	5
CD19	Rat	PE	115508	Biolegend	2.5
CD8	Rat	APC	100712	Biolegend	2.5

Table 2: List of antibodies used for FACS staining (Continued)

Antibody	Host	Conjugate	Catalogue #	Company	Dilution (ug/ml)
CD4	Rat	Alexa Fluor® 700	100430	Biolegend	2.5
CD4	Rat	PE/Cyanine7	100528	Biolegend	2.5
CD11b	Rat	Alexa Fluor® 488	101217	Biolegend	2.5
CD11b	Rat	Alexa Fluor® 700	101222	Biolegend	2.5
CD11b	Rat	APC/Cyanine7	101226	Biolegend	2.5
Ly6G	Rat	APC/Fire™ 750	127652	Biolegend	2.5
Ly6C	Rat	Brilliant Violet 785™	128041	Biolegend	1.25
Ly6C	Rat	PE	128008	Biolegend	1.25
CXCR2	Rat	PE	149304	Biolegend	2.5
F4/80	Rat	Brilliant Violet 421™	123137	Biolegend	2
MHCII	Rat	Alexa Fluor® 488	107616	Biolegend	2.5
Zombie Aqua Fixable Viability Kit	-	BV-510	423101	Biolegend	1:200
7AAD viability staining solution	-	PerCP-cy5-5	420404	Biolegend	1:100

4.1.4 List of materials, kits used and suppliers

All chemicals or kits used in different techniques are shown in Table 3.

Table 3: List of materials used and suppliers

Chemicals	Company	Catalog #
Lung dissociation kit-mouse	Miltenyi Biotec	130-095-927
D-Luciferin	Sigma	2591-17-5
isoflurane	Baxter	FDG9623
Bright-Glo™ Luciferase Assay System	Promega	E2610
RNeasy® Plus Mini Kit	Qiagen	74134 and 74136

4.1.5 List of antibodies used for immunocytochemistry

Table 4 shows the list of antibodies used for immunocytochemistry

Table 4: List of antibodies used for immunocytochemistry

Antibody	Host	Reactivity	Catalog #	Company	Dilution
Ki67	rabbit	Anti-mouse	ab21700	Abcam	Pre-diluted
CD31	rabbit	Anti-mouse	ab28364	Abcam	1:1000
Signal stain boost IHC		Anti-rabbit	8114S	Cell signaling	Pre-diluted

4.2 Methods

4.2.1 Breast cancer cell line

Murine mammary gland cell line 4T1 were a generous gift from Dr Jo Van Ginderachter (Vrije Universiteit Brussel, Belgium) and the genetically engineered 4T1-Luc2 cells to constitutively express the firefly luciferase protein was a generous gift from Dr. Janet V. Cross (University of Virginia School of Medicine, USA). Cells were grown in DMEM supplemented with 10% FBS (Gibco-ThermoFisher Scientific) at 37°C in a humidified atmosphere with 5% CO_2. For implantation experiments, 4T1 cells were trypsinized, washed, resuspended in PBS to a single cell suspension, counted, and unless otherwise indicated $20x10^3$ cells were injected subcutaneously within 30 min. For qRT-PCR, $1.5x10^6$ cells were seeded in 6-well plates and treated with vehicle or 1,10,100 μM Ambrisentan for 4 and 24 hours. Cells were collected in trizol for RNA extraction.

4.2.2 Ambrisentan preparation

Ambrisentan powder, a generous gift by Dr Gabriela Riemekasten (University of Lübeck, Germany) was prepared in solution at a concentration of 20 mg/1ml in distilled water (dH_2O). Since Ambrisentan is poorly soluble in water, 100 mg of the powder was diluted in 2 ml dH_2O adjusted to a high pH (> 12). When Ambrisentan was completely dissolved, HCL was used to decrease the pH to ~7 in the stock solution to a final concentration of 20 mg/ml. Stock was aliquoted in eppendorf tubes and kept in -20°C until use. Before each experiment, a working solution with a final concentration of 1 mg/ml for animal use was also prepared by diluting the 20x stock in dH_2O when needed. Each mouse received 0.2 mg/200 μl of Ambrisentan solution

(equivalent to 10 mg/kg of body weight) by oral gavage P.O. Control animals received an equivalent volume of dH_2O (200 ul). Ambrisentan treatment or water for the control were administered daily for 5 consecutive days, followed by a 2-days break, and this cycle was repeated for a total of 5 weeks, three weeks before tumor implantation, followed by 2 weeks of treatment after the implantation.

4.2.3 Experimental protocol

Female BALB/c mice with matched age and weight were randomly divided into two groups. First group received 200 µl of water daily by P.O and served as control. Second group received 0.2 mg/200 µl of Ambrisentan P.O. and served as treated group. After three weeks of treatment, 4T1 cells (2×104) cells in 100 µl volume, unless otherwise indicated) were orthotopically implanted by injecting the cells subcutaneously into the fourth mammary fat pad following Pulaski et al. protocol (Pulaski & Rosenberg, 2000). Treatment with Ambrisentan or dH_2O was continued for another 2 weeks post implantation. Tumor growth was followed by quantitative determination of tumor volume twice weekly and tumor volume was calculated from two tumor diameter measurements using the following formula: tumor volume = (length×width^2)/2. Mice were sacrificed at day 21 post-implantation, blood was collected, and spleen, tumor, liver and lungs excised for further analysis. For survival experiments, mice were implanted orthotopically with 4T1 cells ($5×10^3$ cells per mouse), tumor volumes were measured twice/week and animal survival was monitored for up to 60 days. Animals with any sign of morbidity including, lethargy, weight loss, hyperkyphosis and piloerection, were humanely sacrificed by CO_2 asphyxiation.

4.2.4 Spleen tissue processing

At the end of experiment, mice were sacrificed, spleens were collected, and single-cell suspension was prepared by mechanical dissociation. Spleens were teased apart into a single-cell suspension by using the frosted ends of two microscope slides using 5 ml of PBS. Red blood cell lysis was performed using 1 ml of RBCs lysis buffer (NH4Cl, KHCO3, and 5% EDTA). The resultant cells were counted manually using a hemocytometer and processed for flow cytometry.

4.2.5 Lung tissue processing

Lungs were excised at the end of the experiment, washed with PBS, cut into small pieces that were transferred into GentleMACS C-tubes (Miltenyi Biotec,Germany), for processing using a lung dissociation kit and a GentleMACS dissociator (Miltenyi), according to the manufacturer's instructions. To obtain a single-cell suspension, homogenized lungs were passed through a 70-mm nylon mesh. The resultant cells were counted manually using a hemocytometer and processed for flow cytometry

4.2.6 Blood processing for single-cell suspension

Blood was collected from animal immediately after scarification to prevent coagulation. Then, 2 ml of 1x RBC lysis buffer was added to each tube and immediately vortexed. Samples were incubated at room temperature for 10-15 the minutes in dark and then centrifuged at 350 g for 5 minutes. Supernatant was aspirated and cells resuspended.

4.2.7 Flow cytometry

0.5x10^6 cells/well from isolated cells were incubated in U shaped bottom 96-well plate (BD) for 30 minutes at 4°C in 50 μl of staining buffer containing anti-CD16/CD32 monoclonal antibody (clone 2.4G2) to block the FcII/III receptors and, therefore, prevent any non-specific binding of the antibodies. Then, the plate was spun at 900 rpm for 5 minutes at 4°C, decanted, and cells incubated with zombie antibody for exclusion of non-viable cells. Afterwards, the plate was spun at 900 rpm for 5 minutes at 4°C, decanted and cells incubated at 4°C for 30 minutes with different combinations of conjugated monoclonal antibodies (Biolegend as detailed in Table 2) in a total volume of 100 μl/well. Then, plates were spun, decanted and cells washed twice with staining buffer, 200 μl/well. Finally, cells were re-suspended in 200 μl of staining buffer and either immediately read or fixed overnight by adding 100 μl of 4% paraformaldehyde. Data were collected on 30,000 cells using BD FACS Celesta (BD biosciences, Mountain View, CA, USA) and analyzed using FlowJo TM software.

4.2.8 Liver tissue fixation and H and E staining

At the end of the experiment, livers were excised and immediately fixed in 10% Formalin. After overnight fixation, tissues were placed in histological cassettes, dehydrated with a series of alcohols, 70% to 95% to 100%, cleared with xylene and then infiltrated and embedded in paraffin (Sherwood Medical, St. Louis, Mo, USA). Using Shandon Finesse 325 manual microtome (Thermo Scientific, Pittsburg, PA, USA), paraffin blocks were trimmed, 5 μm sections prepared and placed on gelatin coated slides. The process of rehydration was done at room temperature by immersing the sections in xylene I solution for 5 minutes, xylene II for 5 minutes, absolute ethanol

I for 3 minutes, absolute ethanol II for 3 minutes, 90% ethanol for 3 minutes, 80% ethanol for 3 minutes and finally 70% ethanol for 3 minutes. Then tissue was stained with Instant Haematoxylin (Thermo Scientific Shandon, Pittsburg, PA, USA) for 10 minutes followed with eosin yellowish (Panreac, Spain) for 1 minute. Finally, the sections were dehydrated in ascending series of graded ethanol, cleared in xylene and mounted with DPX (Panreac, Spain). Images were captured with an Olympus BX51 microscope model V-LH100HG (Olympus Corporation, Japan).

4.2.9 Assessment of liver metastasis

Quantification of micro-metastases, defined as single-to small clusters of tumor cells, in the liver was done using the H and E-stained sections and visualized in a stereo investigator system (Zeiss Imager M2AX10, Germany). For each section, total area was scanned and measured. Digital images were used to quantify the number of tumor metastatic foci in each section and calculated as the number of foci per mm^2 area. To detect the highly proliferative cells, indirect immunostaining with a rabbit anti-mouse Ki67 antibody (Abcam, Cambridge, UK) followed by anti-rabbit-HRP (Cell signaling, Danvers, MA, USA) was used. Antigen retrieval was performed by placing the tissue slides at 200°C for 10 minutes, and then cooled down for 30 mins on ice. Peroxidase activity was determined using DAB chromogen (Dako, Carpinteria, CA, USA). Hematoxylin was used as counterstain, then sections were visualized and photographed with an Olympus BX51 microscope. All slides were examined by a certified pathologist under blinded conditions.

4.2.10 CD31 immunohistochemistry staining and tumor vascularity assessment

At the end of the experiment tumors were collected and fixed with 10% formalin, embedded in paraffin and used to prepare 5 um sections. After tissue dehydration, antigen retrieval was performed by placing the tissue slides at 200°C for 10 minutes, and then cooled down for 30 mins on ice. Endogenous peroxidase activity was blocked using 3% H_2O_2 solution diluted in methanol. After 3 wash cycles with 0.01% Tween-20 in TBS (TBST) (10 minutes each), the slides were further blocked with 5% BSA in PBS for 45 minutes followed by incubation at 4°C with a rabbit anti-mouse CD31 antibody (Abcam, Cambridge, UK) diluted in BSA (1:1000). After overnight incubation, slides were kept for one hour at room temperature, washed and then, incubated with the secondary antibody anti rabbit HRP (Cell Signaling, Danvers, MA, USA) for 30 minutes in a humid chamber at room temperature. After 3 wash cycles with TBST (10 minutes each) the peroxidase activity was determined using DAB chromogen (Dako) for 5-10 minutes followed by wash with distilled water. Sections were then, stained for 1 minute with hematoxylin and dehydrated. dehydration was in the following order: 70% ethanol for 1 minute, 80% ethanol for 1 minute, 90% ethanol for 1minute, absolute ethanol I for 1minute, absolute ethanol II for 1 minute, xylene I for 2 minutes and xylene II for 2 minutes. Finally, sections were mounted with DPX (Panreac, Spain) and images captured with an Olympus BX51 microscope model V-LH100HG (Olympus Corporation, Japan). For tumor vascularity quantification 10 random HPF were scanned, and the blood vessels number and area were recorded. Tumor vascularity was calculated as average surface vessels area per HPF.

4.2.11 Lung metastasis assessment

Lungs were collected at the end of the experiment and the right, and the left lungs were processed separately, and their weight were recorded. Lungs were homogenized in 2 ml DMEM media while the tubes kept on ice at all time to maintain high cell viability. When the tissue homogenate was made to solution, samples were serially diluted, and 100 µl of each dilution was taken and labelled. All samples were in duplicates. Equal volume of the Bright-Glo™ Luciferase Assay reagent (100 µ) (Promega, Madison, USA) was added to each sample. After 5 minutes, samples were vortexed, and the luciferase signal was measured as the relative luminescence level using GloMax®-Multi Detection System (Promega, Madison, USA). Using a protocol that was stablished in the lab, metastatic tumor cells in the lung were quantified as number of metastatic tumor cells per mg of lung tissue.

4.2.12 In vivo bioluminescence imaging (IVIS)

Mice were treated with either dH_2O or Ambrisentan as described in the treatment protocol and implanted with $20x10^3$ 4T1-Luc cells. Prior to imaging, animals received an intraperitoneal injection of D-Luciferin firefly (Sigma) at a dose of 150 mg/kg body weight. 10 minutes after Luciferin injection to ensure consistent photon flux, animals were initially placed in a chamber where they inhaled a mixture of the anesthetic isoflurane (Baxter, Deerfield, IL, USA) and oxygen. Afterwards, mice were moved to the platform in the imaging chamber where their noses were put at the anesthetic-gas ports to maintain anesthesia. At different time points, starting from the day of implantation and followed with once weekly until the end of the experiment, mice were imaged to follow tumor growth and metastasis using the in vivo imaging

system Lumina II (Caliper Life Sciences, Hopkinton, MA, USA). Data acquisition and analysis were performed using living image software (Caliper Life Sciences).

4.2.13 Quantitative RT- PCR analysis

RNA was extracted by trizol method and re-purified on Qiagen columns (RNA easy mini kit, Qiagen, Valencia, CA). The quality and quantity of the RNA was determined using the Nanodrop ND-1000 spectrophotometer (Thermo Scientific, Waltham, MA). cDNA was synthesized using Taqman reverse transcription reagents (Applied Biosystems, Foster City, CA) using manufacturer's protocol. Premade TaqMan primers and probes (Applied Biosystems) were used to study the expression of a set of genes, HPRT (Mm01545399_m1), CXCL1 (Mm04207460_m1), CCL5 (RANTES) (Mm01302427_m1), Mmp9 (Mm00442991_m1), MCP-1 (CCL2) (Mm00441242_m1) and VEGFa (Mm01281449_m1). Transcript levels of target genes were normalized according to the ΔCq method to the respective mRNA levels of the housekeeping gene HPRT. The expression of the target gene is reported as the level of expression relative to HPRT.

4.2.14 In ovo tumor growth assay

Fertilized White Leghorn eggs were incubated at 37.5°C and 50% humidity for 9 days. At the embryonic day 9 (E9), the chorioallantoic membrane (CAM) was dropped by drilling a small hole through the eggshell into the air sac, and a 1cm2 window was cut in the eggshell above the CAM. Cancer cells were trypsinized, washed with complete medium, and suspended in PBS. A 50 µl inoculum of 1×10^6 cells was added onto the CAM of each egg, in a total of 10 to 15 eggs per treatment condition

(to get sufficient surviving embryos at the end of the experiments). Two days later, tumors that began to be detectable were treated every second day at E11, E13, E15, and E17 by dropping 100 μl of the vehicle (PBS) or Ambrisentan (10 mg/kg). At E18, the upper portion of the CAM was removed, washed in PBS, and then the tumors were carefully cut away from normal CAM tissues and weighted to determine the impact of Ambrisentan on tumor growth. The in ovo 4T1-Luc xenografts assay was done by Dr. Samir Attoub's lab (UAE University, Al Ain. UAE) and according to the protocol approved by the animal ethics committee at the United Arabs Emirates University. The eggs were randomly assigned to the treatments, but the experimenter was not blinded to the identities of the groups. All data collected were used in statistical analysis.

4.2.15 Statistical analysis

Statistical significance between control and treated groups was analyzed by unpaired two-tailed Student's t-test or two-way ANOVA test to analyze the difference in tumor volume between the two groups through the different time points. While the log rank (Mantel-Cox) test for Kaplan-Meier functions was used for survival experiments analysis. All tests were performed using GraphPad Prism software (San Diego, CA, USA). Differences between experimental groups were considered statistically significant when P-values were < 0.05.

Chapter 5: Results

5.1 Myelopoiesis is a hallmark of the 4T1 breast cancer model

4T1 is a triple negative murine breast cancer cell line that recapitulate the properties of human TNBC in being highly tumorigenic, invasive and capable of readily metastasizing from the primary tumor to distant organs including the lungs, brain and liver. One of the main characteristics of 4T1 tumor cells is their ability to induce myelopoiesis in the bone marrow through their high level of constitutive production of monocyte chemoattractant protein-1 (MCP-1) and other chemokines (DuPre et al., 2007). As a consequence of this central property, increased accumulation of myeloid cells in the tumor tissue as well as metastatic organs is consistently observed in mice harboring 4T1 tumor cells. Therefore, first the cellular changes in the blood and spleen tissue were analyzed at different time points after 4T1 implantation. Kinetic analysis of blood and spleen tissue of 4T1 tumor-bearing mice was performed. Females BALB/c mice were subcutaneously implanted with $1x10^5$ 4T1 cells and then sacrificed at different time points (Day 14, 21, 28 and 35) post-tumor implantation. Spleen and blood cells were collected, and 6-color flow cytometry was used to study the distribution of myeloid cell populations. Total myeloid cells were identified using the pan-myeloid cell marker CD11b. Myeloid cells which were also positive for the Ly6G cell surface marker were identified as granulocytes. 4T1 tumors resulted in a massive increase in the total myeloid cell population (CD11b+) as early as day 14 post tumor implantation, reaching up to ~80-90% of the total leukocytes in the blood and spleen by day 35 post implantation (Figure 1B, D). Moreover, those cells were predominantly Ly6G+ granulocytes (Figure 6C, E).

Increased granulopoiesis correlated with the significant splenomegaly observed in 4T1 tumor-bearing mice (Figure 6F). The average spleen weight was approximately 3-fold and 6-fold larger than normal at day 21 and 35 post implantation.

5.2 No gross adverse effects observed following Ambrisentan administration in mice

In order to monitor Ambrisentan toxicity in mice, body weight was determined in animals treated with Ambrisentan or vehicle control daily for 3 constitutive weeks. Baseline body weights were recorded just before starting the treatment and at weekly intervals after treatment with either vehicle or Ambrisentan. The percentage change in body weight from baseline was then calculated. Results showed that treatment with Ambrisentan over a 3 week-period did not retard the normal weight gain and treated mice had the same rate of increase in body weight as normal mice (Figure 7A). In another experiment, mice were treated with Ambrisentan daily for two weeks, after which spleens and blood were collected and 6-color flow cytometry was used to examine the effect of Ambrisentan on immune cell populations. Phenotype-specific markers, such as CD19, CD3 and CD11b, were used to identify B cells, T cells and myeloid cells, respectively. The findings confirmed that Ambrisentan treatment did not change the cellular landscape in spleens of treated mice (Figure 7B-D) and did not alter spleen weights. In the blood, however, there was evidence of a decrease in of a decrease in the percentage of myeloid cells in treated animals (Figure 7H). However, the absolute myeloid cell number in both normal and Ambrisentan-treated mice was the same (Figure 7I).
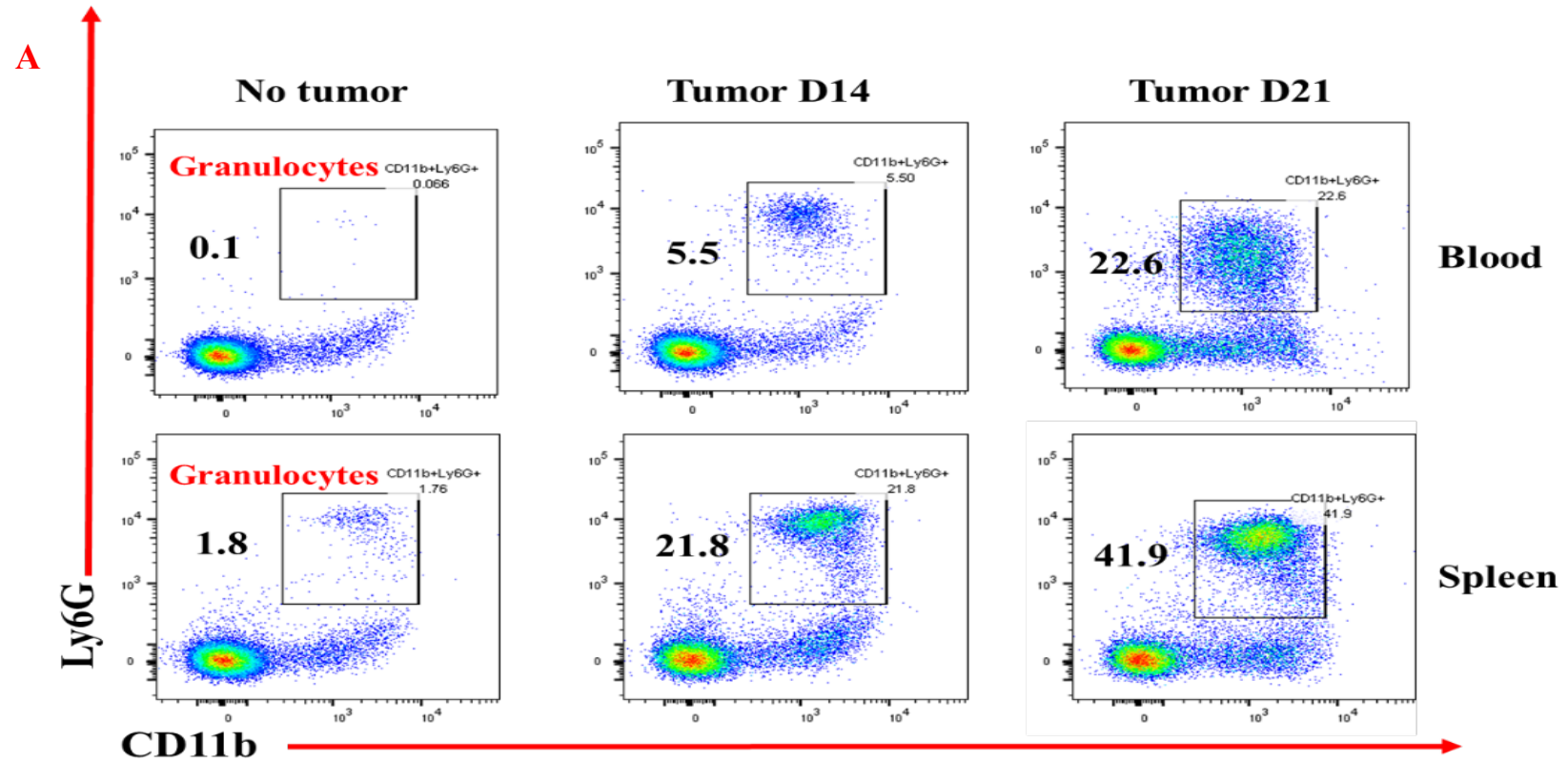
Figure 6: 4T1 tumors promote the accumulation of granulocytes in blood and spleen. Mice were implanted with 4T1 cells, sacrificed at different time points thereafter, as indicated, at which blood and spleens were collected and analyzed by flow cytometry
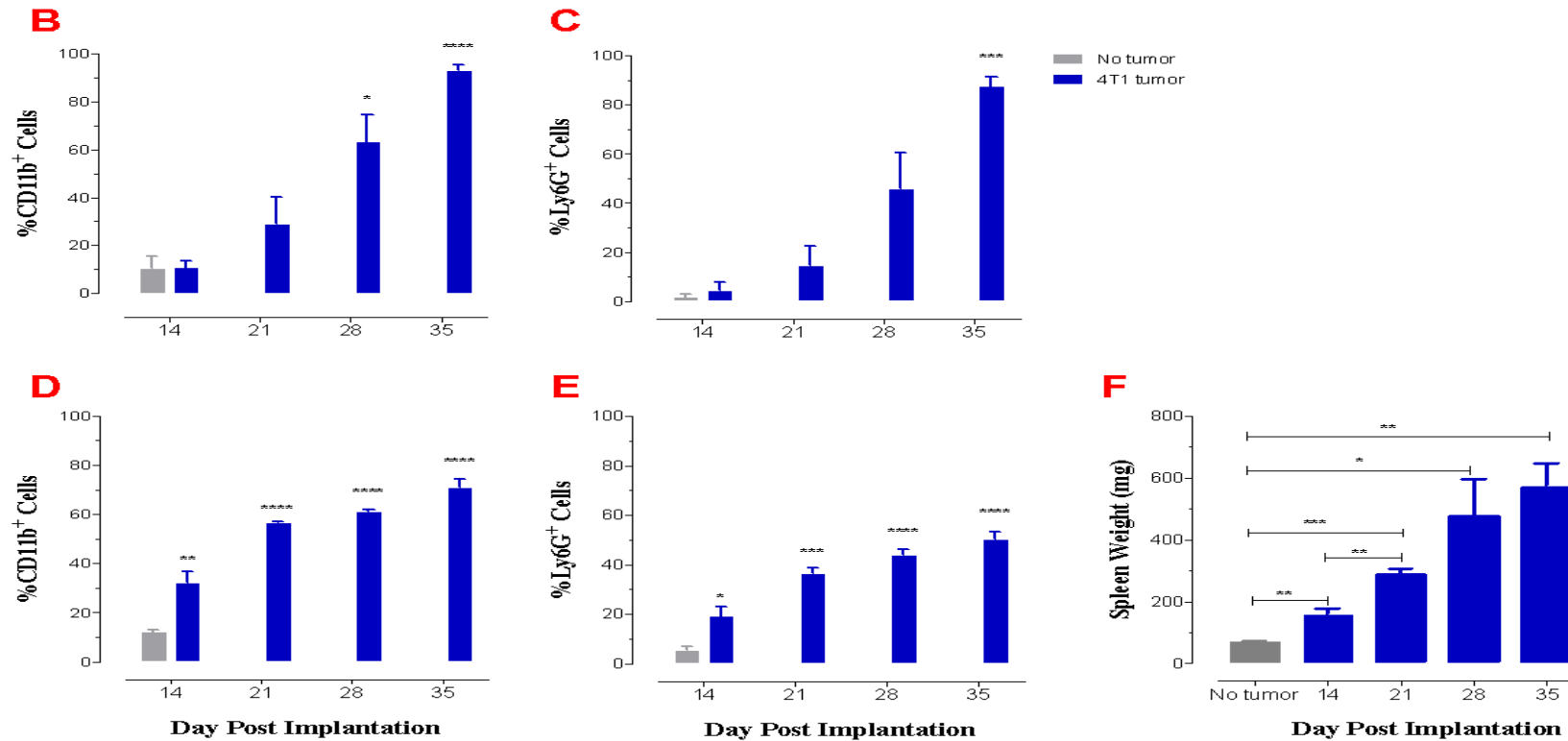
Figure 6: 4T1 tumors promote the accumulation of granulocytes in blood and spleen. Mice were implanted with 4T1 cells, sacrificed at different time points thereafter, as indicated, at which blood and spleens were collected and analyzed by flow cytometry to determine distribution of myeloid cell populations (continued). (B-E) Percentage of CD11b+ cells in blood (B) and spleen (D) showing the accumulation of myeloid cells over time. Those cells were mainly of granulocytic (Ly6G+) phenotype in both blood (C) and spleen (E). Spleen weights of normal or tumor-bearing mice at different time points post 4T1 implantation. Asterisks denote statistically significant differences (* $p < 0.05$, ** < 0.01, *** <0.001). The data is pooled from 3 independent experiments (n = 3-4/group).
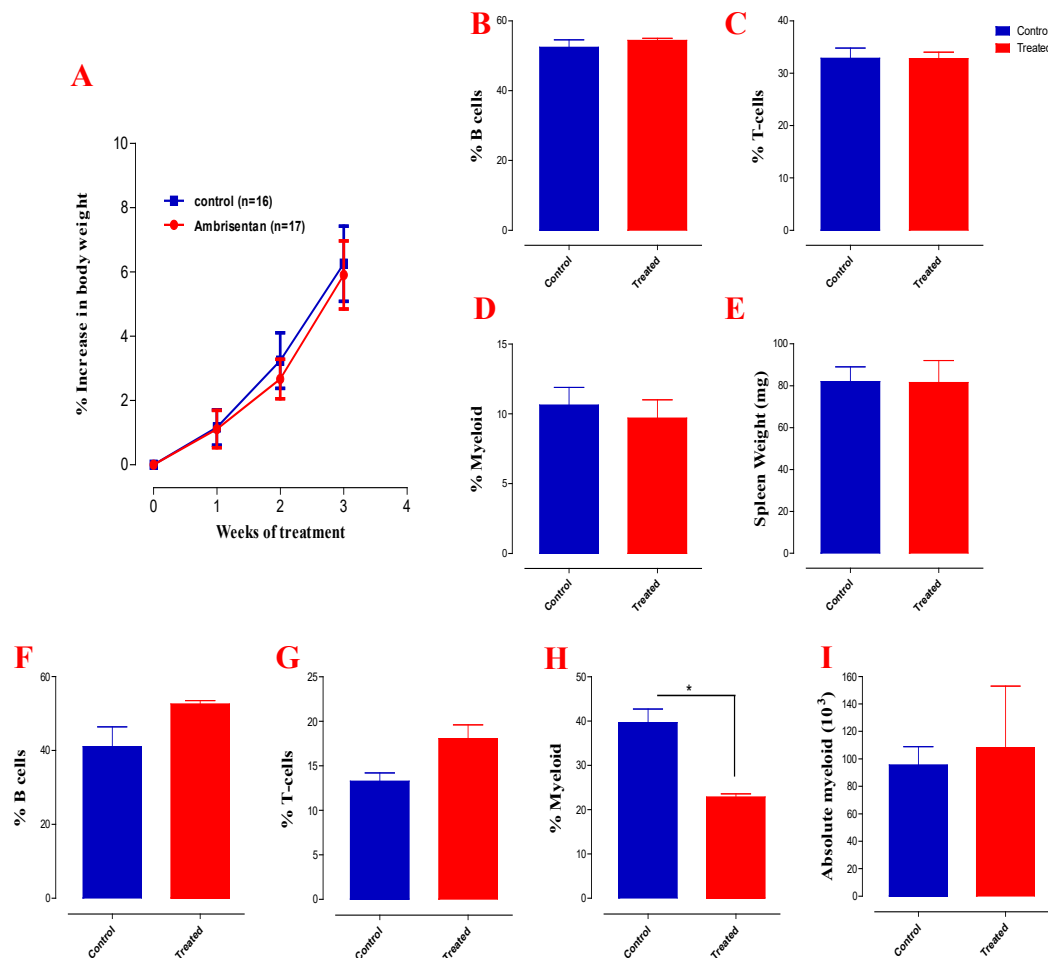
Figure 7: Ambrisentan treatment does not lead to any gross alterations in body weight and immune cell populations in peripheral lymphoid organs. (A) Percentage of increase in body weight in mice treated with Ambrisentan or vehicle (water). Percentage of the different immune cell populations in the spleen (B-D), spleen weight (E), percentage of different immune cell populations in the blood (F-H), and absolute myeloid cells number in the blood (I). Asterisks denote statistically significant differences (* p < 0.05). Data in (A) is pooled from 2 experiments (B-I) from one experiment (n = 3 / group).

5.3 Ambrisentan retards tumor growth in a dose and time-dependent manner

To assess the potential of Ambrisentan as an anti-cancer agent, a preclinical syngeneic mouse 4T1 breast cancer model that express ETAR was used (Kappes et al.,

2020). First, given that Ambrisentan has been approved for use in patients with PAH at 5-10 mg/kg dose (Galiè et al., 2008; Kingman et al., 2009), this study assessed oral administration of Ambrisentan at 5-10 mg/kg dose range in mice. BALB/c mice were given either Ambrisentan or vehicle (control) for 2 weeks, then implanted with 20×10^3 4T1 and treatment continued for another 2 weeks, as illustrated in the schematic treatment protocol shown in Figure 8A. Daily administration of Ambrisentan at 5 mg/kg/day had no apparent effect on the growth of 4T1 tumors (Figure 8B). However, increasing the dose to 10 mg/kg/day led to approximately 55% reduction in primary tumor volume compared to untreated mice at 3 weeks post implantation (Figure 8C).

When the length of treatment prior to tumor implantation was increased to 3 weeks, Ambrisentan led to a significant inhibition in primary tumor growth, reaching ~67% at 3 weeks post implantation, in comparison with controls (Figure 8D). In addition to its effect on tumor growth, Ambrisentan treatment delayed the onset of tumor growth, as shown by its effect on tumor incidence, which is the number of mice with observable tumor (Figure 8E). Based on these findings, the latest protocol of Ambrisentan treatment was used for all subsequent studies.

5.4 Ambrisentan improves host survival in orthotopically‑implanted 4T1 tumor model

Next, the effect of Ambrisentan administration on long-term host survival was evaluated. Following a 3-week pre-treatment with Ambrisentan, mice were inoculated with 5000 4T1 cells after which tumor volume (Figure 9A) and animal survival (Figure 9B) were followed up to 2 months. The overall survival of tumor-bearing animals improved significantly after Ambrisentan treatment. The median animal survival increased from 46 days in the control group to 56 days in Ambrisentan-treated mice.
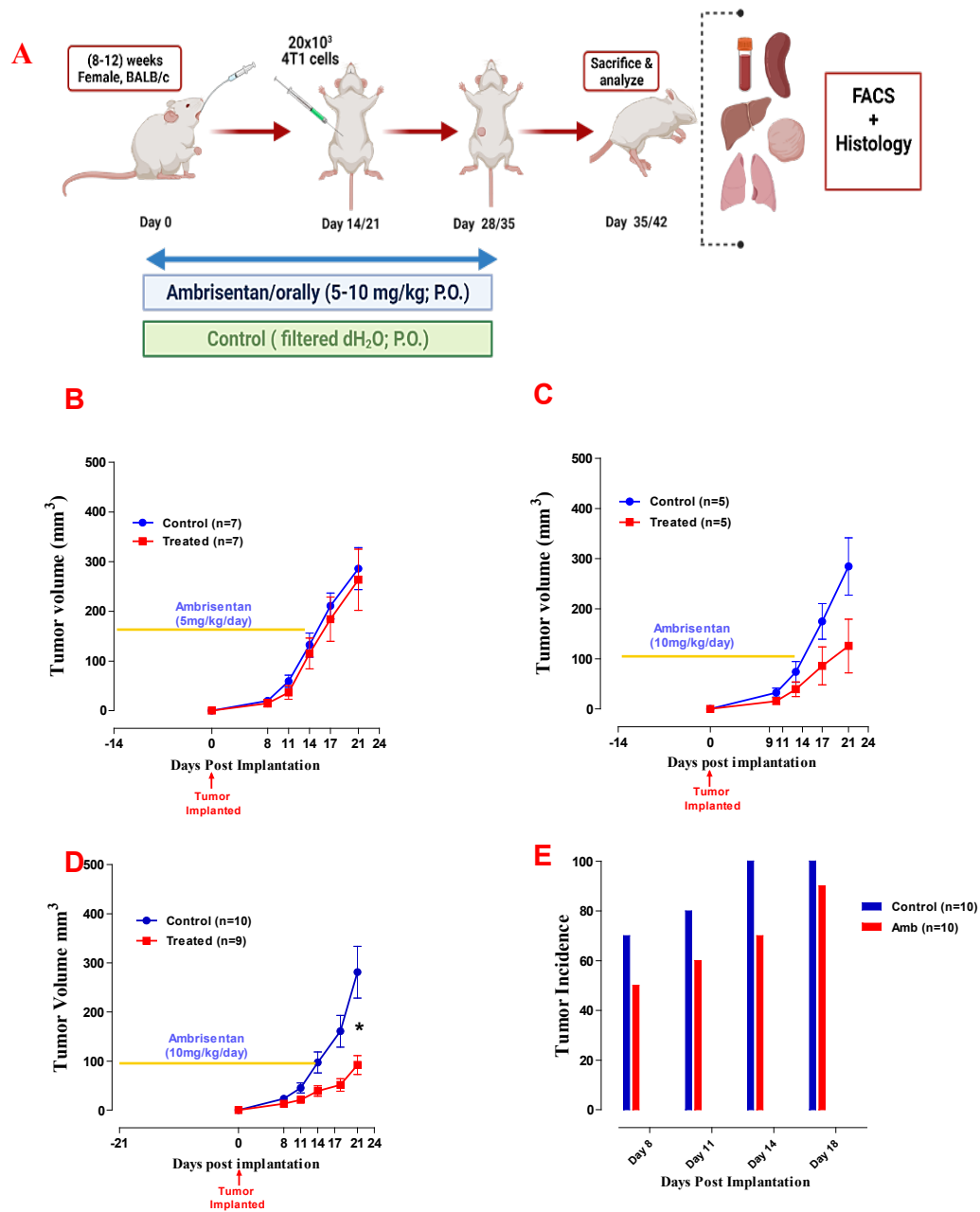
Figure 8: Ambrisentan retards 4T1 tumor growth in a dose and time-dependent manner. (A) Schematic diagram of the treatment protocol for orthotopically-implanted 4T1 breast tumor cells. Oral treatment with Ambrisentan was initiated 2 or 3 weeks prior to 4T1 cell implantation and continued for another 2 weeks post implantation. Unless otherwise indicated, all animals were sacrificed on day 21 post implantation and organs/tissues were collected and processed for the indicated analysis. Effect of Ambrisentan administration using a dose of 5 mg/kg/day (B), or 10 mg/kg/day (C) on tumor growth. Effect of pre-treatment with 10 mg/kg Ambrisentan for 3 weeks on tumor volumes (D) and incidence (E). Numbers in parenthesis denote the number of mice per group for each experiment. Asterisks denote statistically significant differences ($p < 0.05$). The data is representative of 2-3 independent experiments.

Increased from 46 days in the control group to 56 days in Ambrisentan-treated mice.

It is important to note that 4T1 cells are quite aggressive and that due to their highly

metastatic nature, all mice from both groups eventually succumb.
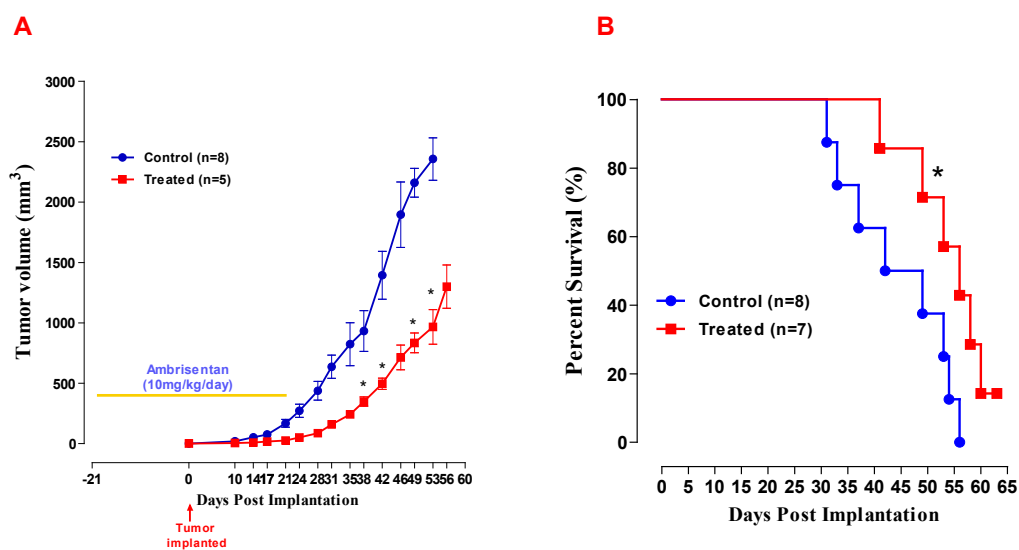
Figure 9: Increased survival after Ambrisentan treatment. Effect of Ambrisentan treatment on tumor growth (A) and host survival (B) after orthotopic implantation of $5x10^3$ 4T1 breast tumor cells. Ambrisentan was administered as shown in Fig. 3A. Animal survival was followed for up to 60 days. The number of mice per group is shown in parenthesis. Asterisks denote statistically significant differences ($p < 0.05$). The data is representative of 2 independent experiments (n= 12-15/group). T-test was used to test the difference in tumor growth between the two group in each time point, while chi squared (Mantel-Cox) statistical test was used for the survival assay.

5.5 Ambrisentan retards tumor growth and metastasis, - in vivo imaging (IVIS) studies

In Vivo Imaging (IVIS) is a sensitive optical imaging system that uses the full

wavelength spectrum from high energy blue to low energy infrared of bioluminescent

and fluorescent reporters. It can be used to track tumor growth and metastasis in

animals in real time. IVIS collects the emitted light signal from the living tissue and acquires a photographic image of the animal under white light and a quantitative bioluminescent signal which is overlaid on the image (Lim et al., 2009). In order to track the growth and metastasis of tumor cells, 4T1-Luc cells have been used which are genetically engineered to constitutively express the firefly luciferase (luc) gene. When 4T1-Luc tumor bearing-mice are injected with luciferin, tumor cells emit a visual light signal that can be monitored and measured using the IVIS Spectrum life imaging system (Lim et al., 2009). Primary tumor growth can be monitored and measured by quantitating the tumor photon flux, which is proportional to the number of light-emitting cancer cells. Similar to the parental 4T1 cell line, growth of 4T1-Luc tumor cells was retarded by oral treatment with Ambrisentan (Figure 10A). In these studies, tumor-bearing mice were imaged once weekly starting on the day of implantation. As shown in the images captured on day 21 post-implantation (Figure 10B), control mice (upper panel) exhibited more robust tumor growth than their Ambrisentan-treated counterparts (lower panel). The bioluminescence signal at the primary tumor implantation site was quantified for each animal and used as an indicator of tumor growth. The data collected from IVIS showed a 5.3-fold reduction in tumor growth in Ambrisentan-treated mice (Figure 10C). Moreover, live imaging was also used to detect metastasis to central organs, such as liver and lungs, by focusing on the appropriate location and covering the implantation site, thereby unmasking the expectedly weaker signals associated with metastatic lesions, as illustrated in Figure 11A. Mice treated with Ambrisentan had 18.3-fold reduction in bioluminescence at tumor metastatic sites (Figure 11B).
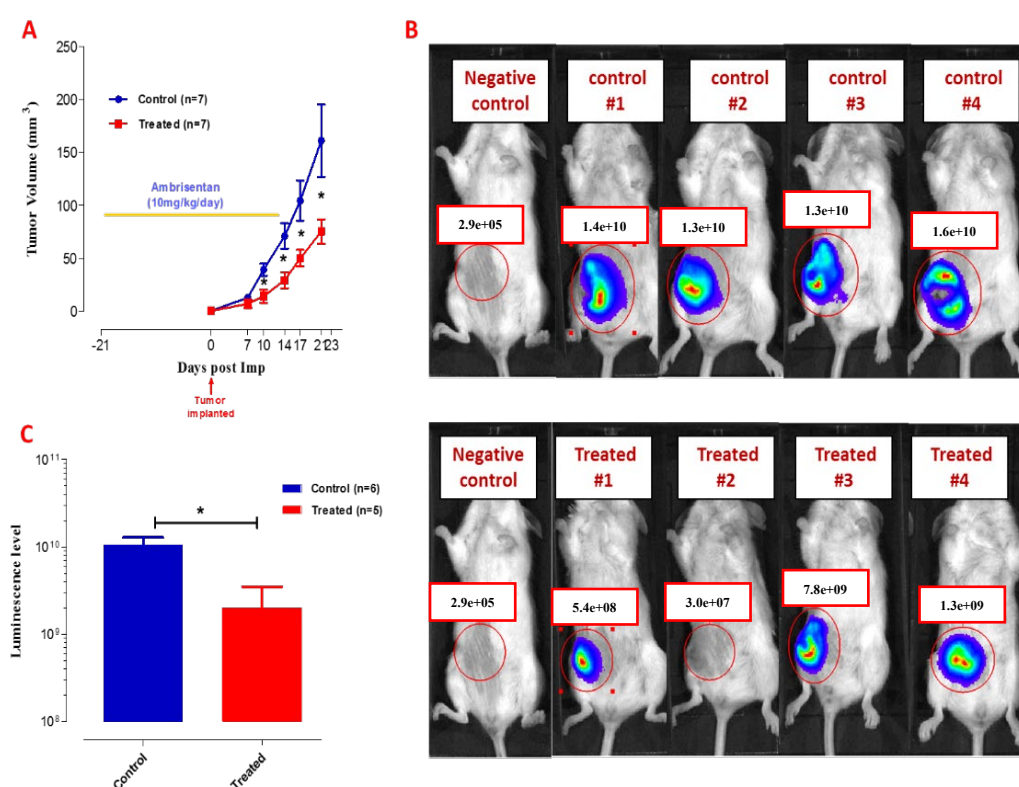
Figure 10: Growth of breast tumors detected by in vivo imaging of luciferase-labeled 4T1 tumor cells. Mice were orally gavaged with either water only (control) or Ambrisentan (at 10 mg/kg/day) for 3 weeks, implanted with 4T1-luc cancer cells, and continued treatment for another 2 weeks post implantation. (A) 4T1-Luc2 tumor growth with and without Ambrisentan treatment. (B) Representative images of tumor-bearing animals, control (top) or Ambrisentan-treated (bottom) were captured on day 21 post implantation. (C) Bioluminescence signals associated with the site of tumor implantation (indicated by red circles in B) were determined and used as an indicator of tumor growth. Number of mice per group is shown in parenthesis. Asterisks denote statistically significant differences ($p < 0.05$). The data is representative of 2 independent experiments (n=15-18/group).

5.6 Inhibition of liver tumor metastasis in Ambrisentan treated mice

4T1 triple-negative breast cancer cells are well known to continuously metastasize to the lung and liver (Stormes et al., 2005). To examine the effect of Ambrisentan administration on the extent of 4T1 metastasis to the liver, liver tissues were collected 3 weeks post tumor implantation. Tissue sections were fixed, stained

and the whole section was scanned under the microscope to determine the total number of tumor metastatic foci. Liver foci count was then calculated per section area. Ambrisentan-treated mice had significantly fewer metastatic foci (~ 43% reduction) compared to vehicle controls (Figure 12A–F). These foci appeared clearly as small aggregates of tumor cells (Figure 12A, C) and stained strongly with anti-Ki67 antibody (Figure 12B, E), indicating a high proliferative state. The tumor foci had the characteristics of malignant cells including high nuclear/cytoplasmic ratio, irregular contour, and abnormal mitotic figures (Figure 12C).
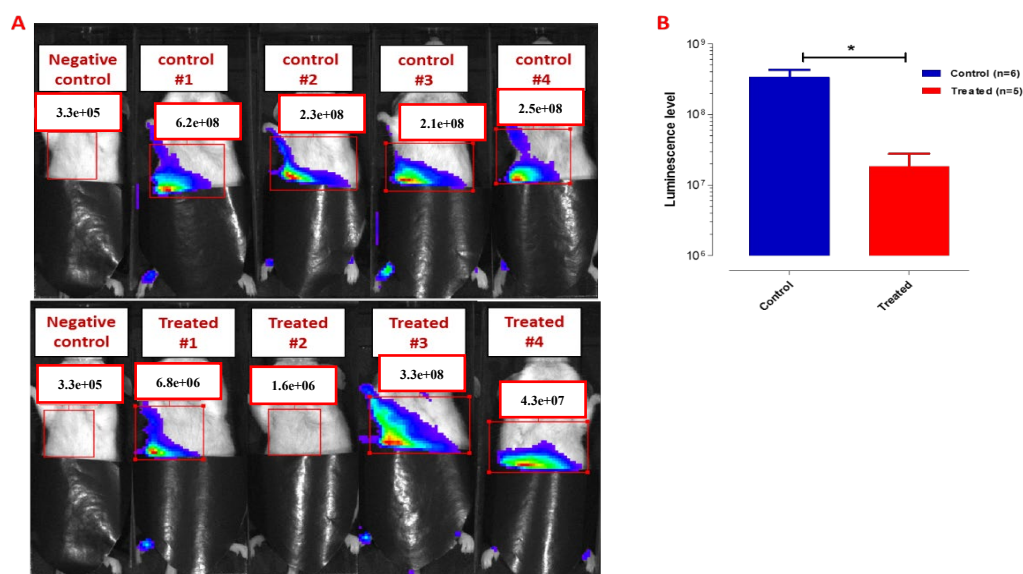
Figure 11: Detection and quantification of tumor metastasis to distant organs in mice implanted with luciferase-expressing 4T1 breast tumors. (A) Representative mice from either untreated (top panel) or Ambrisentan-treated (bottom panel) group are shown. Images were obtained after masking the signal from the implantation site and focusing on the metastatic upper body regions. Images were captured on day 21 post implantation. (B) Bioluminescence signals associated with the metastatic site (indicated by red rectangles in A) were determined and used as an indicator of metastasis. Number of mice per group is shown in parenthesis. Asterisks denote statistically significant differences (p < 0.05). The data is representative of 2 independent experiments (n=15-18/group).
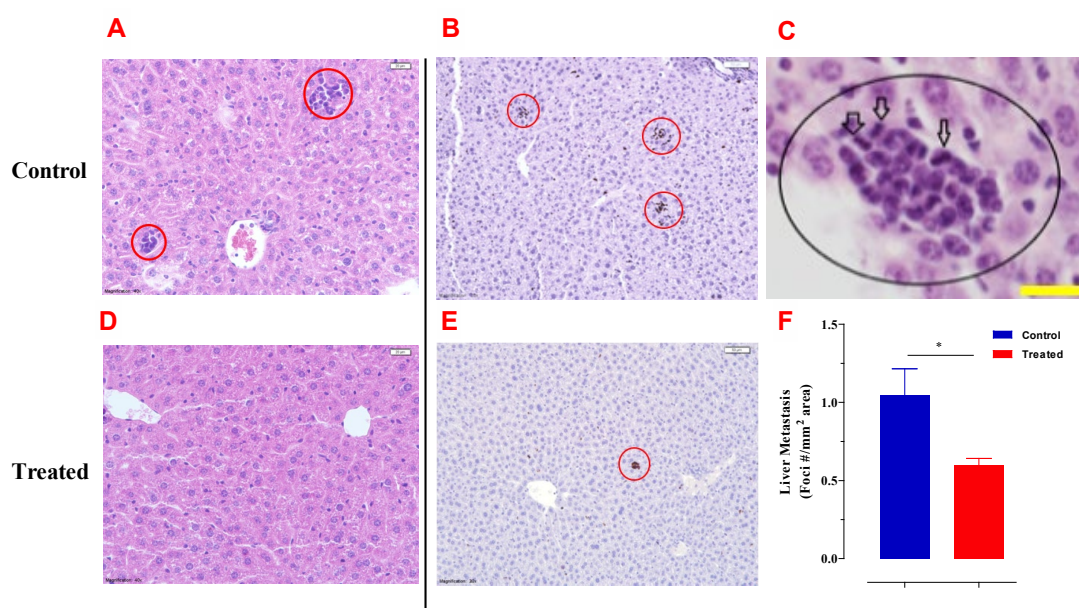
Figure 12: Assessment of liver metastasis in 4T1 breast tumor-bearing mice after Ambrisentan administration. (A-F) Liver tissues were collected 3 weeks post implantation of 4T1 tumor cells and sections were prepared and processed for H and E (A, C, D) and Ki67 (B, E) staining. Images taken at 40 × (A, D), 60 × (C) or 20 × (B, E) magnification are shown. Representative liver sections of control (A-C) or Ambrisentan-treated (D, E) mice are shown. Tumor metastatic foci consisting of a small cluster of tumor cells, strongly Ki67-positive, are circled in red. Arrows (C) indicates proliferative malignant cells (F) The number of metastatic foci was determined for representative liver sections and calculated per mm2 area. Asterisks denote statistically significant differences (p < 0.05). The data is representative of 3 independent experiments (n = 11–12 / group).

5.7 Reduced tumor growth correlates with decreased myelopoiesis

As shown in Figure 6, orthotopic implantation of 4T1 cells in the fat mammary pad resulted in the accumulation of granulocytes (CD11b+Ly6G+) in the blood and spleen. Assessment of myeloid cell infiltration in the lungs was used as a correlate to the extent of 4T1 tumor metastasis. Mice were treated with either vehicle (water) or Ambrisentan (10 mg/kg/day), as shown in Figure 8A. At day 21 post implantation, mice were sacrificed, and spleen, lung and blood were collected for flow cytometric

analysis. Representative dot plots illustrating the gating strategy used for spleen cells are shown in Figures 13 and 14 (a similar gating strategy was used for the analysis of blood and lung tissue). Two different antibody panels were used, one for the phenotypic characterization of hematopoietic cell populations (Figure 13), while the second focused on analysis of the different myeloid subpopulations (Figure 14).
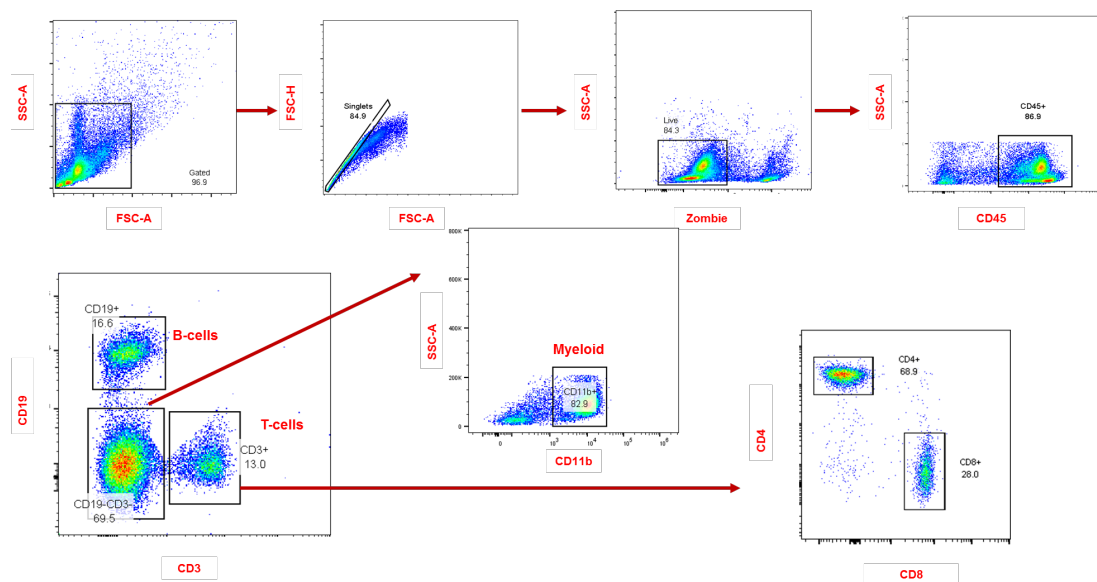
Figure 13: Gating strategy for spleen hematopoietic cells. After the exclusion of doublets, debris, and non-viable cells, immune cells were identified using the pan-hematopoietic marker CD45+ cells were further analyzed for B cells and T cells using their markers CD19+ and CD3+ respectively. T cells were analyzed for CD4 and CD8 positivity. Cells that were negative for CD3 and CD19 markers were further gated for the myeloid cell marker, CD11b+. The same gating strategy was used for the lung and blood.
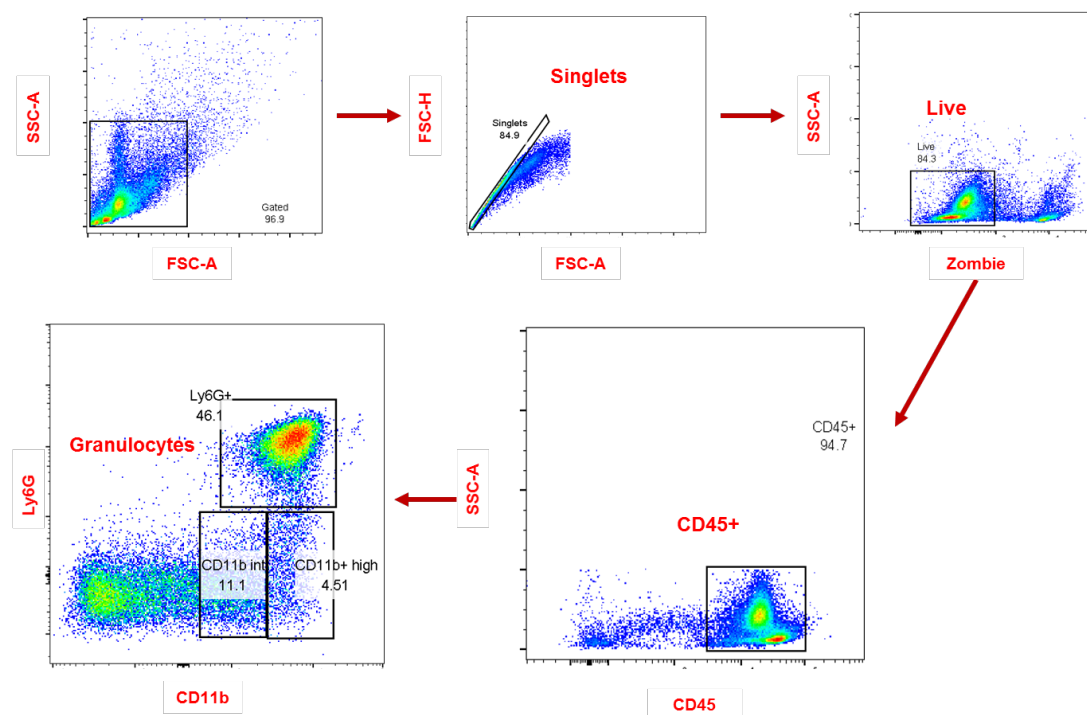
Figure 14: Gating strategy for spleen myeloid cells. After the exclusion of doublets, debris, and non-viable cells, immune cells were identified using the pan-hematopoietic marker CD45. CD45+ cells were further analyzed for Ly6G+CD11b+ cells, which count for granulocytes, CD11b-intermediate (CD11b-int) and CD11b-high cells. The same gating strategy was used for the lung and blood.

Based on their positive expression of CD11b, the majority of the gated CD45+ cells in the blood, spleen and the lungs of 4T1-bearing mice are of myeloid origin, with an average of ~78%, 53% and 54%, respectively. Ambrisentan treatment led to a significant decrease in myeloid cells in the blood, spleen and lung, averaging ~35%, 18% and 63%, respectively (Figure 15 A-F). The myeloid cells can be broadly subdivided into Ly6G-positive (granulocytes) or negative (monocytes) subpopulations. Further analysis using myeloid cell-specific panel of antibodies confirmed that the majority of CD11b+ cells are granulocytes. Pre-treatment with Ambrisentan significantly reduced the accumulation of granulocytes by 40% and 26%

in the blood and spleen, respectively. Similarly, there was a significant decrease in hematopoietic cell infiltration into the lungs of treated mice that was accompanied by a 69% reduction in granulocyte accumulation. The observed reduction in granulocytic infiltration in the lungs most likely reflects decreased 4T1 cell metastasis to these organs. In Figure 15, FACS dot plot representing CD45+, myeloid cells and granulocytes are shown (Figure 15A-C). Moreover, as a result of decrease in myeloid cells population in the spleen, Ambrisentan treated mice have a significant ~26% reduction in spleen weight compared to untreated (Figure 15F).

5.8 Ambrisentan impairs metastasis to the lung

Further confirmation of the ability of Ambrisentan to inhibit tumor metastasis to the lungs was carried out by quantifying the bioluminescence signal in lung tissue after implantation with 4T1-Luc cells. Three weeks post implantation, lungs were collected from control or Ambrisentan-treated mice, homogenized in 2ml DMEM media to prepare single cell suspension and processed for luciferase signal detection, using the Bright Glo Luciferase Assay System. Since tumor cells are the sole source of any bioluminescence signal detected in the lung tissue, the extent of metastasis is proportional to the measured relative luminescence level. Luciferase signal was determined for each sample and standardized to 1×10^6 lung cells (Figure 16). Lungs in the treated group had ~94% reduction in bioluminescence signal compared to control lungs (Figure 16A). To quantify the approximate number of metastatic tumor cells in the lung, a standard curve of the bioluminescence level of a specific number of 4T1-Luc cells (10, 100, 1000, and 10,000) taken directly from in vitro culture or mixed with lung cell suspension was stablished (Figure 16B). Using the standard curve, the approximate number of metastatic 4T1 cells in normal mice was 635 cells per mg lung

tissue. In sharp contrast, extent of metastasis was reduced by 97.8% to 14 cells/mg in Ambrisentan-treated mice (Figure 16C). The findings underscore the potent inhibitory effect of Ambrisentan on tumor metastasis in this preclinical model of triple-negative breast cancer.
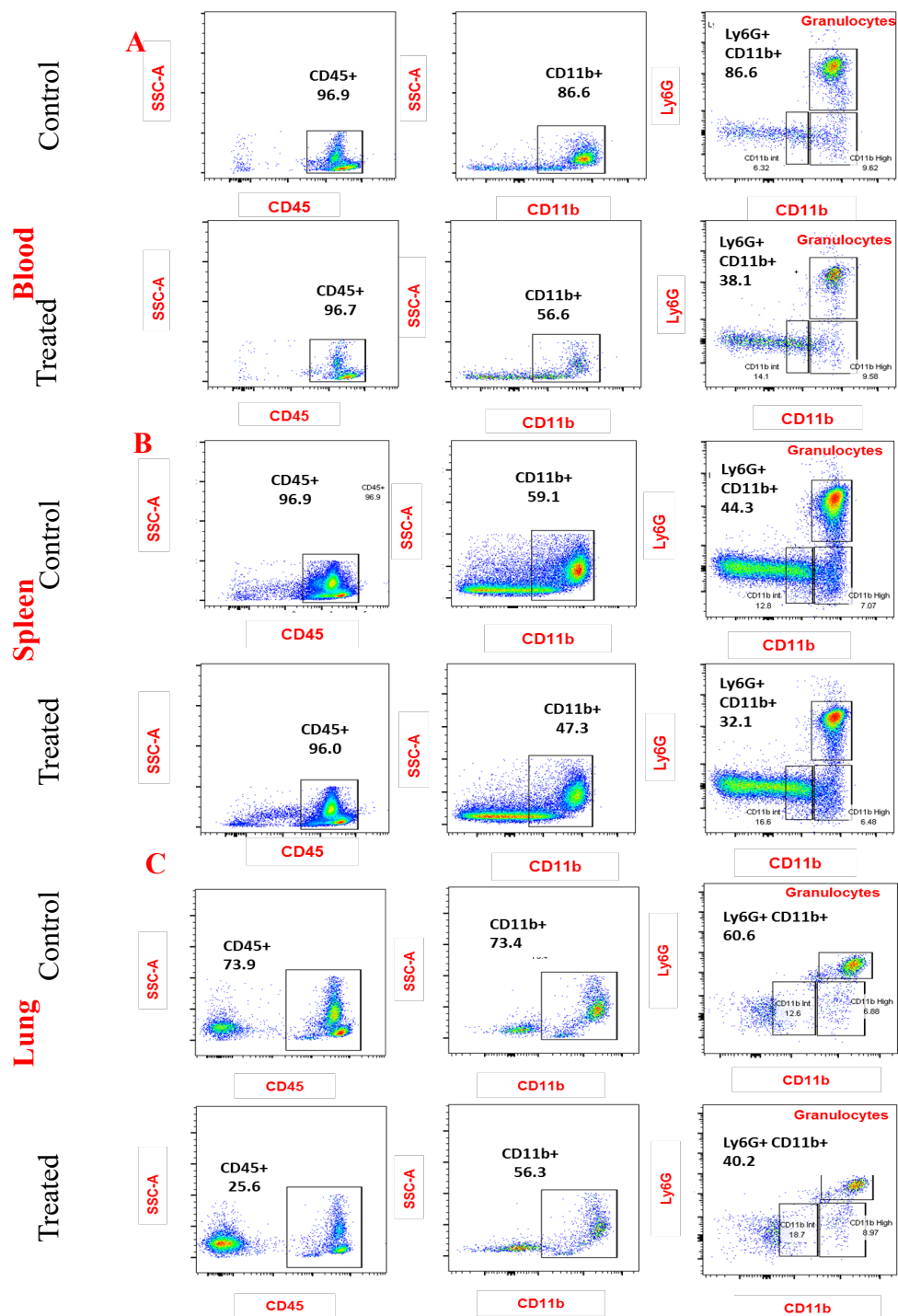
Figure 15: Ambrisentan retards myeloid cell accumulation at secondary sites. (A-C) representative FACS gating of mouse blood (A), spleen (B) and lung (C) tissue. For each organ, CD45+ cell was gated (left most dot plot) from which CD11b+ cells are selected (middle dot plots). Right hand dot plots illustrate the staining profiles with antibodies for CD11b and Ly6G cell surface markers. In each sub-figure (A-C), the upper panel represents control mice and lower panel represents Ambrisentan-treated mice.
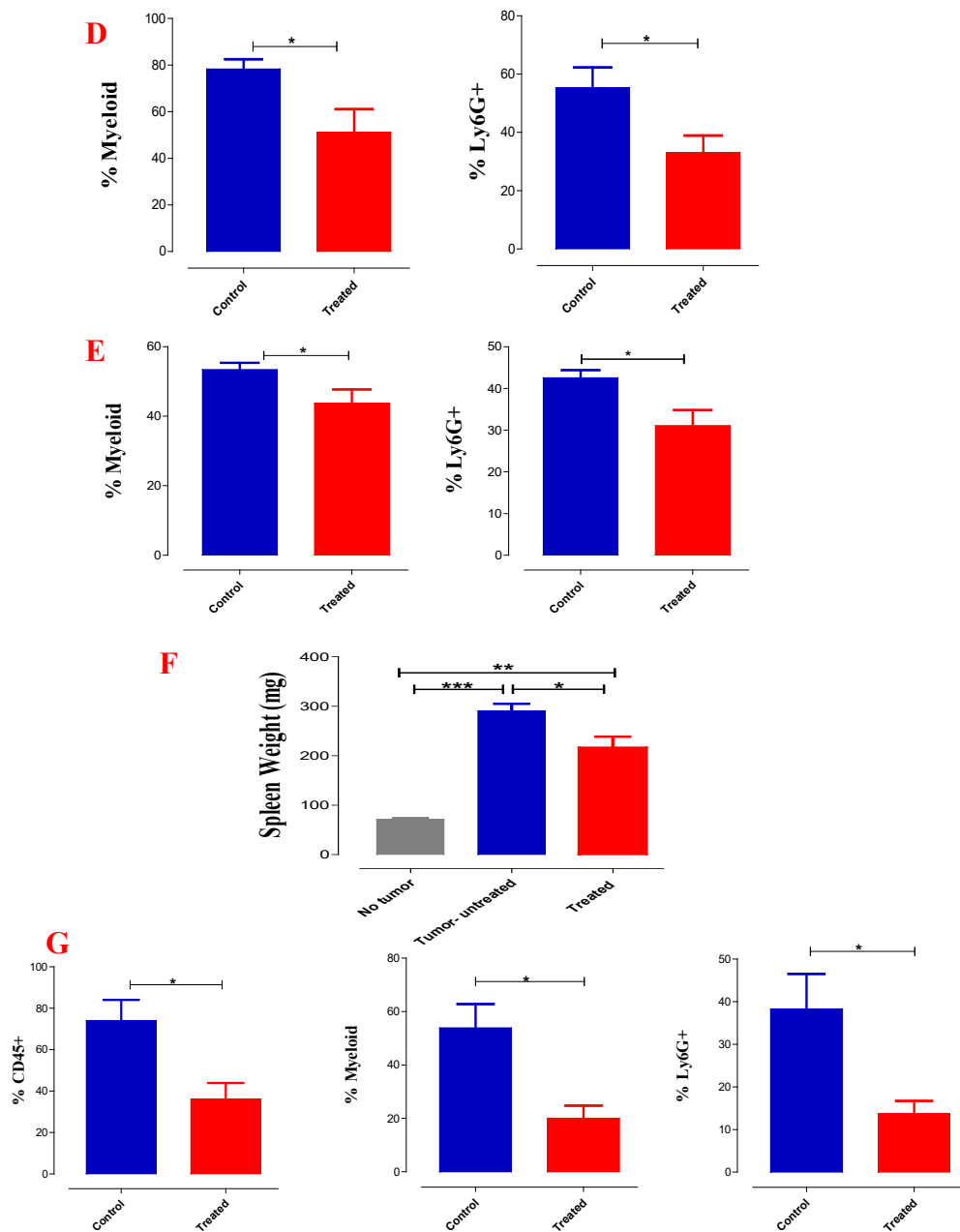
Figure 15: Ambrisentan retards myeloid cell accumulation at secondary sites (Continued). (D, E, G) Quantification of total myeloid (CD11b+) cells and granulocytes (Ly6G+) in the blood (D), spleens (E) and lungs (G) of tumor-bearing mice. Alterations in spleen weights are shown in (F). Asterisks denote statistically significant differences (* $p < 0.05$, ** $P<0.01$). The data is pooled from 2 independent experiments (n = 6–8 / group).
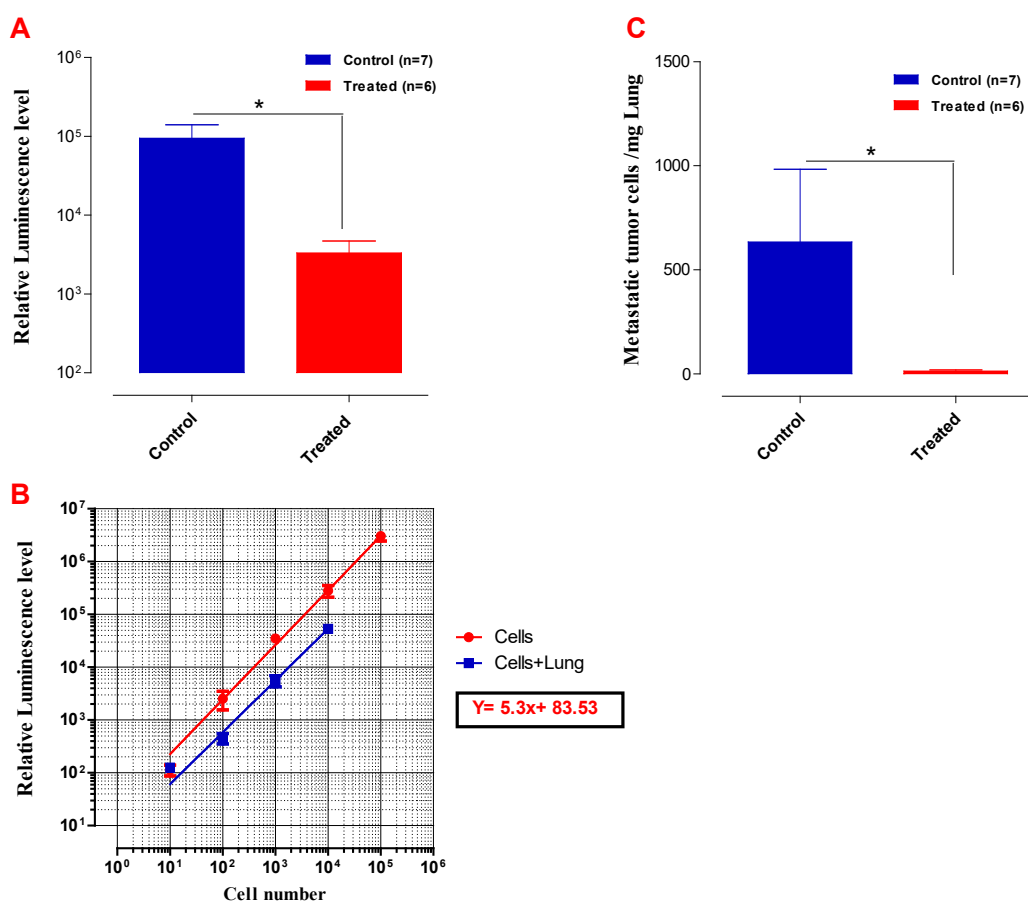
Figure 16: Assessment of lung metastasis in 4T1 breast tumor-bearing mice after Ambrisentan administration. (A-C) lung tissues were collected 3 weeks post implantation of 4T1-Luc tumor cells. Tissues were homogenized in MDEM media, then serially diluted and a total volume of 100µl was taken from each dilution and an equal volume of the Bright Glo reagent was added to the samples. Samples relative luminescence was determined using GloMax-multi detection system. (A) Relative luminescence level per 1×10^6 lung cells was calculated. Treatment with Ambrisentan reduced luminescence signal in treated lungs by $\sim$ 94% compared to control lungs. (B) Relative Luminescence of 4T1-Luc cells alone or mixed with lung cells. The graph indicates 5 folds decrease when 4T1 cells are mixed with lung cells (C) Number of metastatic tumor cells / mg lung for each group was determined using the best fit curve of the signal detected by mixing lung cells with 4T1-Luc cells (blue line in B). The graph indicates $\sim$97% decrease in the number of metastatic tumor cells/mg lung in treated mice. Asterisks denote statistically significant differences, using nonparametric t-test (* $p < 0.05$). The data is pooled from 2 independent experiments (n = 6-7/ group)

5.9 Ambrisentan treatment reduces tumor vascularity

The growth of tumor tissue and ability of tumor cells to metastasize are linked to critical changes in the tumor microenvironment, including angiogenesis and epithelial-to-mesenchymal transition. In many tumors, vascular density can be an indicator of metastatic potential, the higher the vascularity, the higher is the incidence of tumor metastasis (Zetter, 1998). Therefore, tumor tissue of control and Ambrisentan-treated mice were analyzed for changes in angiogenic potential by staining with CD31-specific monoclonal antibody, a specific marker of endothelial blood vessels.

To quantify the data, 10 high power fields (HPF) were randomly scanned for each tissue section and blood vessel number and area were determined. Tumor vascularity was calculated as total vessel area per HPF (μm2/HPF). As shown in Figure 17, a significant reduction in the extent of angiogenesis was observed in tumors of animals treated with Ambrisentan. Total tumor vascularity was reduced by ~55%, mainly due to a decrease in the size of blood vessels (Figure 17E-G).

5.10 Ambrisentan decreased the expression level of CXCL1 and MMP9 in cultured 4T1 cells

To shed light on the potential mechanism of action of Ambrisentan, cultured 4T1 cells were cultured in the presence or absence of Ambrisentan for 4 or 24 hours. After extraction of RNA, gene expression was determined by quantitative RT-PCR. Gene expression profile of important factors, including CXCL1, CCL5, MMP9, MCP-1 (CCL2) and VEGF-A was determined. The expression of these chemokines and growth factors are known to play an essential role in tumor progression and metastasis. This analysis revealed the ability of Ambrisentan to target 4T1 cells directly and

significantly reduced their expression of CXCL1 and MMP9 with a trend of decrease in CCl5 and VEGF-A (Figure 18A-D). However, there was no significant changes in the expression of CCL2 was observed.
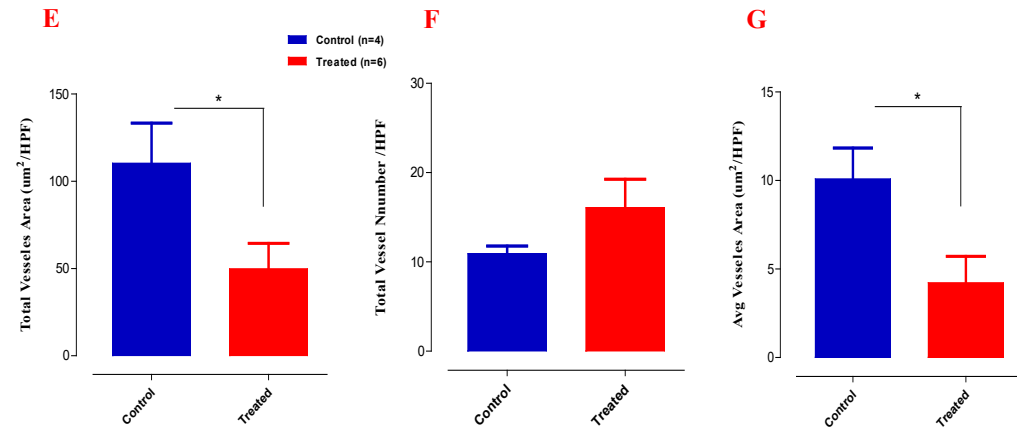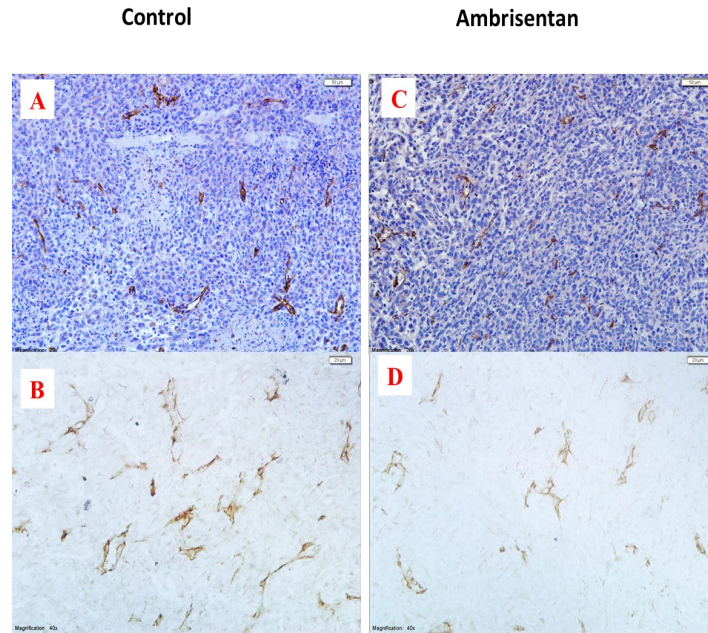
Figure 17: Effect of Ambrisentan treatment on tumor vascularity. (A-G) Tumor tissues were collected 3 weeks post implantation of 4T1 tumor cells and sections were processed for CD31 staining (A- D). Images taken at 40× magnification are shown. Representative tumor sections of control (A, B) or Ambrisentan-treated (C, D) mice are shown, with counterstain (A, C) or without (B, D). (E-G) Blood vessel count was calculated as the mean of counts in 10 fields per section randomly selected from non-necrotic areas of the tumors. Area of each blood vessel in the field was determined and tumor vascularity was calculated as the mean of total vessels area in µm2/HPF. Treatment with Ambrisentan significantly reduced tumor vascularity (E) due to the decrease in vessel area (G). Asterisks denote statistically significant differences ($p < 0.05$). The data is representative of 3 independent experiments (n = 15–20 / group).
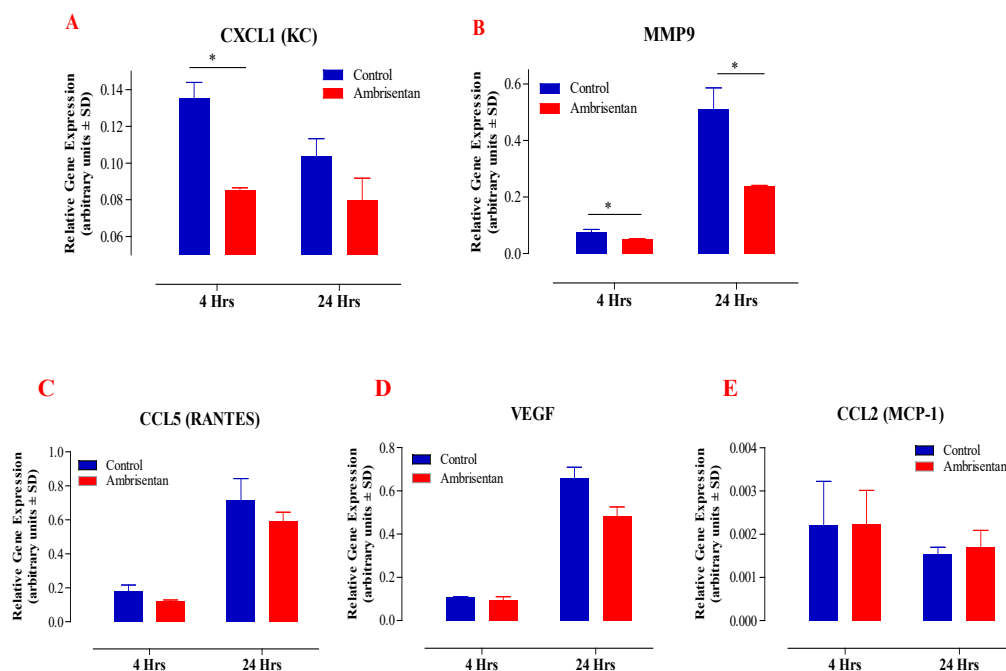
Figure 18: Ambrisentan treatment reduce genes expression level in culture. 1.5×10^6 were seeded in 6 well plate, cells were treated with either vehicle or Ambrisentan for 4 and 24 hours and RNA was extracted for qRT-PCR. Treatment with Ambrisentan significantly decreased (A) CXCL1 and (B) MMP9 mRNA levels with a trend of decrease in (C) CCL5 and (D) VEGF. No significant effect on (E)CCL2. Transcript levels of target genes were normalized according to the ΔCq method to respective mRNA levels of the housekeeping gene HPRT. The expression of the target gene is reported as the level of expression relative to HPRT. Asterisks denote statistically significant differences ($p < 0.05$). The data is representative of 3 independent experiments.

5.11 Treatment with Ambrisentan retards tumor growth in ovo

Independent from the host immune system, the effect of Ambrisentan on tumor growth was investigated in vivo using the in ovo chick embryo tumor growth assay, also known as the Chorioallantoic membrane (CAM) assay. CAM is a structure that can rapidly expands generating a rich vascular network that provides an interface for gas and waste exchange, making it a simple animal model to study tumor formation

and metastasis (Ribatti, 2017). At the embryonic day 9 (E9), CAM was dropped and 1×10^6 4T1-Luc cells were added onto the CAM of each egg. After 2 days, tumors began to be detectable and were then treated with 10 mg/kg Ambrisentan every 2 days (E11, E13, E15 and E17). To prepare 10 mg/kg Ambrisentan dose, fertilized egg at day 11 was weighted and embryo's weight was used to prepare a working solution of Ambrisentan in 1ml saline, then 100 µl was added/egg. At E18, tumors were recovered from the upper CAM and weighed (Figure 19A). Ambrisentan treatment reduced the growth of 4T1-Luc by ~25% (Figure 19B). Toxicity was also evaluated by comparing the number of dead embryos in control and treated groups. At the end of the experiment (E18), Ambrisentan showed no toxic effect as there was no difference in the number of surviving embryos in control and Ambrisentan-treated groups (Figure 19C). These results corroborate previous findings of the inhibitory potential of Ambrisentan on tumor growth independently of possible additional actions on anti-tumor immune responses.
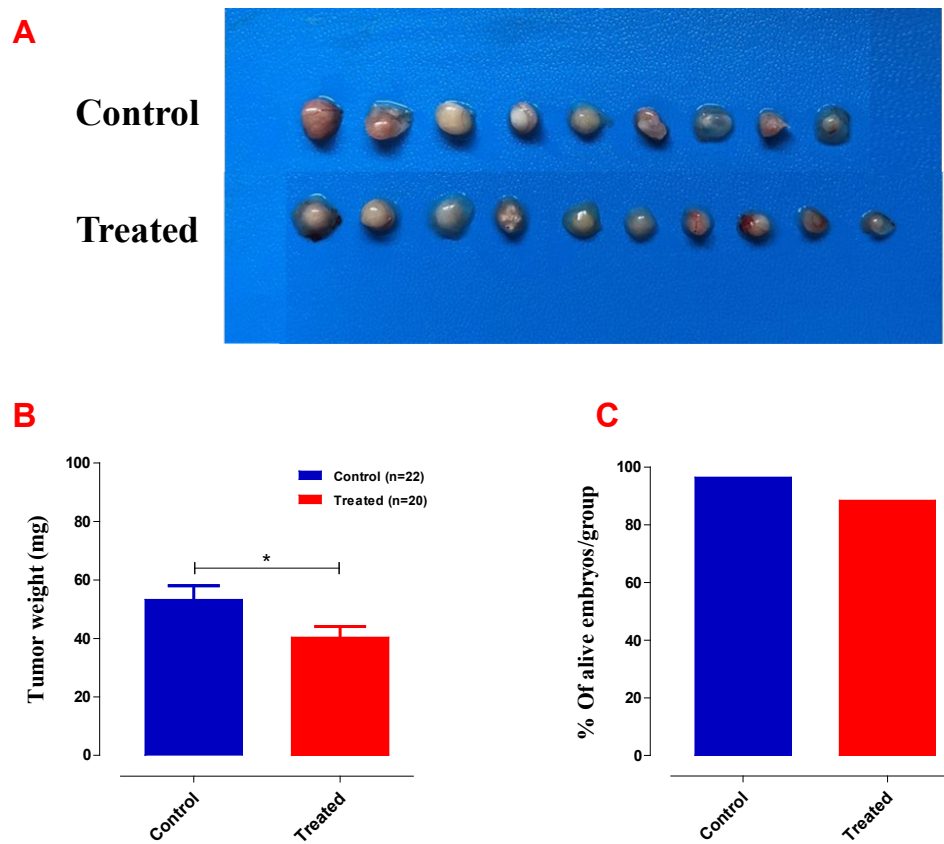
Figure 19: Effect of Ambrisentan on 4T1 tumor growth in ovo. 4T1-Luc2 cells were inoculated at E9 and after two days when tumors were detectable, were treated with 10 mg/kg Ambrisentan every second day, E11, E13, E15 and E17. (A) At day 18, tumors of each group were collected and weighed. (B) Ambrisentan treatment reduced tumor weight by 25% compared to control tumors (C) Treatment with 10 mg/kg Ambrisentan has no cytotoxic effect as there was no difference in the number of surviving embryos in control and treated groups. Numbers in parenthesis denote the number of embryos per group. The data is pooled from 2 independent experiments (n=20-24/group)

Chapter 6: Discussion

The findings of this study show the capacity of Ambrisentan to impair the primary tumor growth of the triple negative 4T1 breast cancer cells and inhibit their metastasis to distant organs, including the liver and lungs. In this study Ambrisentan was used in a preventative model, prior to tumor implantation and was continued for two weeks after the implantation. The advantage of using the preventative protocol, where the drug can be found in the blood before implanting the tumor cells is to help understand the impact of the drug on metastasis, if the drug is capable to block metastasis this will show in the incidence of metastasis in the group. However, the drug can also work by decreasing the growth of metastasis in distant organs rather than blocking it completely, which was observed after Ambrisentan treatment. In addition, this study is considered the first to investigate the effect of ERAs on breast cancer, also the 4T1 TNBC model used in here is highly aggressive and mimics the human TNBC very well and is highly metastatic. Since there is no previous work was done on this model, Ambrisentan was tested on preventative model. Ambrisentan is already approved by the US Food and Drug Administration (FDA) and the European Medicines Agency (EMA) and has an advantage over other ETRAs by the lower reported rates of liver toxicity (Newman et al., 2007). The data reported herein highlight Ambrisentan as a potential therapeutic drug for controlling breast cancer progression and metastasis.

Autocrine and paracrine activation of tumor cells by ET-1-induced signaling elicits pleiotropic effects on progression and metastasis of ovarian, prostate, colon, breast, bladder and lung cancers (Nie et al., 2014; Smollich et al., 2008; Wülfing et al.,

2005). ETAR expression has been shown to be upregulated on breast cancer in comparison with non-neoplastic breast tissue (Nie et al., 2014; Smollich et al., 2008; Wülfing et al., 2005). In addition, there is extensive cross communication between the ET-1 axis and several growth factors, including epidermal growth factor (EGF), vascular endothelial growth factor (VEGF), transforming growth factor beta (TGF-β) and IL-6, all of which being essential factors for tumor growth and progression (Nelson et al., 2003; Rosanò et al., 2013). This makes the ET-1 axis a rational target for cancer therapy.

This project findings are in agreement with previous pre-clinical studies, where the blockade of endothelin receptors using specific antagonists led to a significant tumor growth inhibition and apoptosis induction (Bagnato et al., 1995; Nelson et al., 2003; Nelson et al., 1995). Macitentan, the dual-specific ETAR and ETBR antagonist, was shown to inhibit tumor growth and metastasis in resistant ovarian cancer xenografts in mice (Sestito et al., 2016) and to increase sensitivity to chemotherapy in colorectal cancer- stem cell (CRC-SC) patient-derived xenograft (Cianfrocca et al., 2017). In a recent study, pretreating the human ovarian cancer cells (SKOV3-Luc) with ambrisentan prior to implantation suppressed intraperitoneal seeding and metastasis (Masi et al., 2021). Moreover, the specific ETAR antagonist Zibotentan and the selective ETAR antagonist Atrasentan have demonstrated a potential anticancer activity in preclinical studies in prostate cancer (Bagnato et al., 2011; Morris et al., 2005) and promising outcomes in Phase II trials in patients with advanced metastatic prostate cancer. Phase III trials were carried out in patients with non-metastatic prostate cancer or advanced metastatic prostate cancer using Zibotentan or Atrasentan as monotherapy or in combination with the chemotherapeutic

agent docetaxel (Miller et al., 2013). All trials with established advanced disease have so far failed to demonstrate benefits of ETRs blockade over placebo in the treatment of cancer (Miller et al., 2013; Murphy, 2005), suggesting the need for new therapeutic approaches.

Based on the findings to date, inhibition of tumor metastasis by Ambrisentan is likely to be due to the direct effect of Ambrisentan on tumor cells. data in this project show that gene expression of matrix metallopeptidase 9 (MMP9) and the chemokine CXCL1 (known as KC) is reduced in Ambrisentan-treated 4T1 cells. MMP9 is a significant protease that plays essential role in extracellular matrix (ECM) remodeling through the cleavage of several ECM proteins (Huang, 2018). As a result of its proteolytic activity, MMP9 is involved in the degradation of ECM, alteration of cell-cell and cell-ECM interactions, in addition to the cleavage of cell surface and extracellular proteins (Ortega et al., 2005; Stamenkovic, 2003). Moreover, MMP9 plays a role in basement membrane degradation (Hou et al., 2014), an essential step in tumor development that acts to support tumor invasion and metastasis. At the tumor primary site, MMPs can release soluble factors in the circulation, which in turn can promote the establishment of a metastatic niche in distant organs (Kessenbrock et al., 2010). MMPs are produced by the tumor cells themselves as well as by stromal cells in the tumor microenvironment in response to corresponding stimulatory interactions (Radisky & Radisky, 2007). They are strongly linked to breast cancer aggressiveness and metastasis, hence the overexpression of MMP9 is a characteristic of triple-negative and HER2-positive breast cancers (Yousef et al., 2014). The knockdown of MMP9 on basal-like, triple negative breast cancer cell lines, including BT-549, SUM159PT and MDA-MB-231 cells, significantly suppressed cell invasion in matrigel transwell assay

(Mehner et al., 2014). In addition, none of the mice bearing MMP9-silenced tumors of MDA-MB-231 breast cancer showed pulmonary metastasis, while metastasis to the lung was detected in all the control mice. This finding highlights the importance of tumor cell-produced MMP9 for metastasis in basal-like triple negative breast cancer.

Chemokines are a subset of cytokines which function primarily to direct the migration of leukocytes in response to a chemical gradient of ligand, known as the chemokine gradient (Balkwill, 2004). The chemokine CXCL1 has a crucial role in the host immune response and mainly acts on neutrophils recruitment according to chemokines gradient (Sawant et al., 2016). CXCL1 mediates its function by binding to the G-protein coupled receptor CXCR2. CXCL1 expression has been shown to correlate with lung relapse in breast tumors (Minn et al., 2007; Minn et al., 2005) as well as with increasing the aggressiveness of circulating breast tumor cells (Kim et al., 2009). Additionally, CXCL1 was shown to be upregulated in LM2-4175 breast cancer cells (LM2), which grow aggressively and metastasize to the lungs (Acharyya et al., 2012). The knockdown of CXCL1 by two independent shRNA hairpins in LM2 cells significantly decreased mammary tumor growth and lung metastasis, and induced tumor apoptosis. However, CXCL1 knockdown did not result in any visible changes in angiogenesis or cell proliferation rates in vitro. In the same study, knockdown of CXCL1 significantly reduced CD11b+Gr1+ myeloid cell population within the tumor. These myeloid cells represent a heterogeneous group of cells, including precursors for neutrophils and monocytes, both expressing CD11b and Gr1 (Gabrilovich and Nagaraj, 2009). In mice, Gr1+ cells include granulocytes (Ly6G+) and macrophages (Ly6C+) (Rosenberg and Sinha, 2009). Further characterization of myeloid cells revealed a decrease in the Ly6G+ granulocytes in the tumor and a decrease in both

Ly6G+ granulocytes and Ly6C+ monocytes (Ly6C+) in the lungs of animals bearing CXCL1-negative tumors (Acharyya et al., 2012). These findings highlight the distinguished role of CXCL1 in tumor progression and uncover a network of paracrine signals between tumor, myeloid and endothelial cells that drives tumor progression and metastasis in breast cancer. Considering these previous findings, one can hypothesize that the observed inhibition in tumor progression and metastasis by Ambrisentan can be attributed to its capacity to inhibit the release of pre-metastatic factors by 4T1 breast tumor cells.

The relationship between myeloid cells and 4T1 tumors is very essential for 4T1 tumor growth and progression. The orthotopic implantation of 4T1 cells in the mammary fat pad in mice induces a huge increase in myelopoiesis in the primary tumor site and the metastatic organs (DuPre et al., 2007). In this study, a kinetic analysis of blood and spleen tissue of 4T1-tumor bearing mice showed a massive increase in the granulocytic (Ly6G+) myeloid cell population as early as day 14 post tumor implantation, reaching up to ~80-90% of the hematopoietic cells by day 35 post implantation. The extraordinary alterations observed in the 4T1 breast cancer model suggest that Ly6G+ cells are critical contributors to tumor growth through their secretion of various chemokines and other factors. Cultured 4T1 cells have been shown to express mRNA transcripts for the myeloid cell chemokines RANTES, MCP-1 and CXCL1, MIP-1α and MIP-1β (DuPre et al., 2007). Chemokine secretion by 4T1 cells correlates with myeloid cell accumulation in the primary tumor and plays a crucial role in metastasis to distant organs. Through this capacity, 4T1 cells appear to hijack host myeloid cells, effectively recruiting them to serve the growing tumor. In addition to their role in supporting tumor growth and invasion, several lines of evidence suggest

that these intratumoral myeloid cells can differentiate into cells with an immunosuppressive capacity known as myeloid derived suppressor cells (MDSCs) (Condamine et al., 2015; Marvel & Gabrilovich, 2015). MDSCs can be divided into two main subpopulations, granulocytic Ly6G+ MDSCs (gMDSCs) and monocytic Ly6C+ MDSCs (mMDSCs). In addition to their immunosuppressive activity in cancer patients and tumor-bearing mice, MDSCs play important roles in promoting angiogenesis, invasion and tumor metastasis through the formation of pre-metastatic niches (Condamine et al., 2015). In the invasive 4T1 model, tumor-bearing mice develop spontaneous lung metastasis; in contrast, no detectable metastasis is observed in the lungs of mice bearing the less invasive EMT6 tumor (Ouzounova et al., 2017). In the same study, 4T1 cells induced an infiltration by mMDSCs into the primary tumor tissues and gMDSCs into the lungs of tumor-bearing mice. It is worth noting, however, that no functional assays were done to prove the immunosuppressive capacity of those Ly6G+ cells in the study by Ouzounova et al. Nevertheless, it is important to emphasize that the increase in Ly6G+ cell accumulation in the lungs is entirely consistent with previously published data using the same tumor model (Kappes et al., 2020). In this context, Ambrisentan-mediated inhibition of tumor growth may explain the observed reduction in the percentage of Ly6G+ cells in the lungs of treated mice. Furthermore, the data suggest that Ambrisentan treatment is changing the balance from a pro-tumor microenvironment to one that is more hostile to tumor growth.

This project findings also demonstrate that Ambrisentan treatment decreased tumor vascularity and lead to the production of smaller, presumably less functional, blood vessels. Tumor angiogenesis is the process in which a network of blood vessels

is formed to supply tumors with oxygen and required nutrients to support their growth. Angiogenesis is induced by hypoxia, various growth factors and chemokines (Whipple & Korc, 2010). Within the tumor tissue, the balance between angiogenic stimulators and inhibitors is lost and the release of angiogenic factors and proteolytic enzymes induce the proliferation of endothelial cells and promote the degradation of the basement membrane and ECM (John & Tuszynski, 2001; Whipple & Korc, 2008). This, in turn, increases the likelihood of metastatic spread and growth of metastatic foci in distant organs (Whipple & Korc, 2008). The interactions between tumor cells and host stromal cells in the tumor microenvironment are essential for tumor cell proliferation, invasion, angiogenesis, and metastasis (Liotta & Kohn, 2001). Endothelial cells and fibroblasts are among the most vital components of tumor stroma (Hughes, 2008). Endothelial cells facilitate tumor progression through the release of matrix bound growth factors, such as VEGF and FGFs, in addition to a variety of MMPs, especially MMP 2, 3, and 9, that contribute to ECM degradation and cause the release of additional pro-angiogenic growth factors. Moreover, the important role of chemokine-mediated angiogenesis in tumor growth has been demonstrated in many cancers, including breast cancer, gastrointestinal malignancies, prostate carcinoma, melanoma, renal cell carcinoma, ovarian cancer, glioblastoma, and head and neck cancer (Kitadai et al., 1998; Mestas et al., 2005; Miller et al., 1998; Richards et al., 1997). In melanoma, CXCL 1, 2 and 3 are all highly expressed. Immortalized murine melanocytes that do not form tumors acquire the ability to form highly vascular tumors in vivo after transfection with these chemokines (Owen et al., 1997). Furthermore, depletion of CXCL1, 2, or 3 in the hosts lead to a reduction in tumor-associated angiogenesis and inhibition of tumor growth, underscoring the important roles played by these chemokines in tumor growth.

Recent evidence also has pointed out to another mechanism that Ambrisentan could be acting on metastatic process, mainly by inhibiting invadopodia (Masi et al., 2021). Invadopodia are actin-rich membrane extensions used by cancer cells to degrade the ECM, a non-cellular structure comprising the basement membrane and the collagen-based interstitial matrix

Chapter 7: Conclusion

Ambrisentan treatment significantly reduced tumor growth and improved overall survival of 4T1 tumor-bearing mice. This was correlated with reduction in tumor metastasis to major organs, including liver and lungs. To understand the underlying mechanism for the anti-metastatic effect of Ambrisentan, the extent of angiogenesis within the tumor tissue was examined. The data revealed a significant reduction in the total tumor vascularity in Ambrisentan treated group, mainly due to a decrease in the size of blood vessels, making it insufficient to supply the tumor with the optimal amount of oxygen and nutrients needed for tumor growth. In addition, cultured 4T1 cells treated with Ambrisentan showed a significant decrease in the Matrix metallopeptidase 9 (MMP9) and the chemokine ligand CXCL1, both which are crucial for 4T1 tumor progression and metastasis. Figure 20 is summarizing the main findings of this study. Ambrisentan is seems to act on the tumor cells to make them more immunogenic than cells in the absence of Ambrisentan. Treatment seems to allow more vigorous antitumor immune response, by decreasing the immunosuppressive effect of 4T1 tumor microenvironment and shifting the balance from protumor to antitumor microenvironment. These findings demonstrate a significant and beneficial effect of Ambrisentan in this highly metastatic breast cancer model and provide a rationale for targeting ETAR as a potential adjuvant therapy in cancer patients.

For future studies, therapeutic potential of Ambrisentan in combination with chemotherapeutic agents needs to be investigated. The combination treatment could help to reduce the high mortality rates in breast cancer patients as well as to ameliorate

the overall rate of severe morbidity due to side effects of chemotherapy agents administrated to patients with cancer. Moreover, a better understanding of the mechanism of action of Ambrisentan is needed in order to fully realize the potential of this class of drugs in cancer treatment.
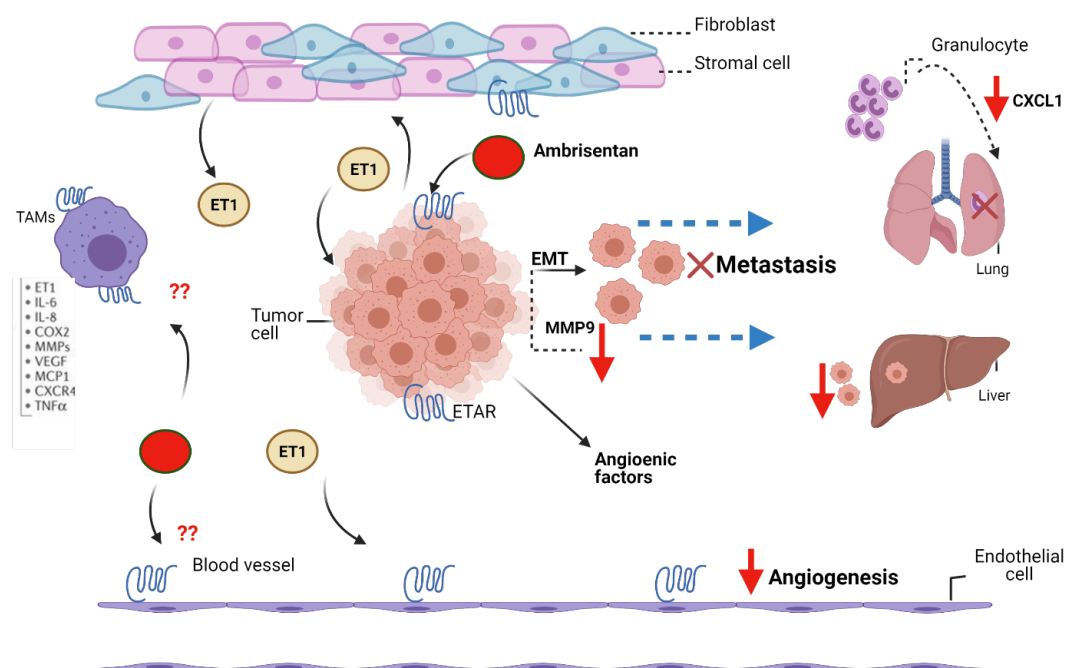
Figure 20: Schematic diagram summarizing the main finding of the study. Tumor environment is a heterogenous mixture of cells including, the tumor cells, stromal cells, fibroblast and immune cells. All are secreting factors can be used by the tumor for its continued growth and metastasis. Ambrisentan treatment blocks metastasis to distant organs such as the lungs and liver. When 4T1 cells were cultured with Ambrisentan. There was a significant reduction in key factors important for metastasis (mmp9) as well as chemokines that recruit granulocyte to the site of tumor growth (cxcl1) showing that Ambrisentan is acting directly on tumor cells. Ambrisentan treatment also decreased the degree of angiogenesis in the tumor tissue by decreasing the size of the blood vessels.

References

Acharyya, S., Oskarsson, T., Vanharanta, S., Malladi, S., Kim, J., Morris, Patrick G., Massagué, J. (2012). A CXCL1 Paracrine Network Links Cancer Chemoresistance & Metastasis. *Cell, 150*(1), 165-178. doi: https://doi.org/10.1016/j.cell.2012.04.042

Allavena, P., Germano, G., Marchesi, F., & Mantovani, A. (2011). Chemokines in cancer related inflammation. *Experimental Cell Research, 317*(5), 664-673.

Aslakson, C. J., & Miller, F. R. (1992). Selective events in the metastatic process defined by analysis of the sequential dissemination of subpopulations of a mouse mammary tumor. *Cancer Research, 52*(6), 1399-1405.

Aubert, J.-D., & Juillerat-Jeanneret, L. (2016). Endothelin-receptor antagonists beyond pulmonary arterial hypertension: cancer and fibrosis. *Journal of Medicinal Chemistry, 59*(18), 8168-8188.

Aysola, K., Desai, A., Welch, C., Xu, J., Qin, Y., Reddy, V., . . . Beech, D. J. (2013). Triple negative breast cancer–an overview. *Hereditary Genetics: Current Research, 2013*(Suppl 2). doi:10.4172/2161-1041.s2-001

Baba, A. I., & Câtoi, C. (2007). Tumor cell morphology *Comparative Oncology*: The Publishing House of the Romanian Academy.

Bagnato, A., Cirilli, A., Salani, D., Simeone, P., Muller, A., Nicotra, M. R., . . . Venuti, A. (2002). Growth inhibition of cervix carcinoma cells in vivo by endothelin A receptor blockade. *Cancer Research, 62*(22), 6381-6384.

Bagnato, A., Loizidou, M., Pflug, B., Curwen, J., & Growcott, J. (2011). Role of the endothelin axis and its antagonists in the treatment of cancer. *British Journal of Pharmacology, 163*(2), 220-233.

Bagnato, A., Rosanò, L., Spinella, F., Di Castro, V., Tecce, R., & Natali, P. G. (2004). Endothelin B receptor blockade inhibits dynamics of cell interactions and communications in melanoma cell progression. *Cancer Research, 64*(4), 1436-1443.

Bagnato, A., Tecce, R., Moretti, C., Di Castro, V., Spergel, D., & Catt, K. J. (1995). Autocrine actions of endothelin-1 as a growth factor in human ovarian carcinoma cells. *Clinical Cancer Research, 1*(9), 1059-1066.

Balkwill, F. (2004). Cancer and the chemokine network. *Nature Reviews Cancer, 4*(7), 540-550.

Banerjee, S., Hussain, M., Wang, Z., Saliganan, A., Che, M., Bonfil, D., . . . Sarkar, F. H. (2007). In vitro and in vivo molecular evidence for better therapeutic efficacy of ABT-627 and taxotere combination in prostate cancer. *Cancer Research, 67*(8), 3818-3826.

Barst, R. J. (2007). A review of pulmonary arterial hypertension: role of ambrisentan. *Vascular Health and Risk Management, 3*(1), 11. doi:10.2147/vhrm.s15026

Barst, R. J., Ivy, D., Dingemanse, J., Widlitz, A., Schmitt, K., Doran, A., . . . van Giersbergen, P. L. (2003). Pharmacokinetics, safety, and efficacy of bosentan in pediatric patients with pulmonary arterial hypertension. *Clinical Pharmacology and Therapeutics, 73*(4), 372-382.

Ben-Baruch, A. (2006). The multifaceted roles of chemokines in malignancy. *Cancer and Metastasis Reviews, 25*(3), 357-371.

Bergmann, C., Strauss, L., Zeidler, R., Lang, S., & Whiteside, T. L. (2007). Expansion and characteristics of human T regulatory type 1 cells in co-cultures simulating tumor microenvironment. *Cancer Immunology, Immunotherapy, 56*(9), 1429-1442.

Bloch, K., Eddy, R., Shows, T., & Quertermous, T. (1989). cDNA cloning and chromosomal assignment of the gene encoding endothelin 3. *Journal of Biological Chemistry, 264*(30), 18156-18161.

Bonano, M., Tríbulo, C., De Calisto, J., Marchant, L., Sánchez, S. S., Mayor, R., & Aybar, M. J. (2008). A new role for the Endothelin-1/Endothelin-A receptor signaling during early neural crest specification. *Developmental Biology, 323*(1), 114-129.

Borsig, L., Wolf, M. J., Roblek, M., Lorentzen, A., & Heikenwalder, M. (2014). Inflammatory chemokines and metastasis—tracing the accessory. *Oncogene, 33*(25), 3217-3224.

Bray, F., Ferlay, J., Soerjomataram, I., Siegel, R. L., Torre, L. A., & Jemal, A. (2018). Global cancer statistics 2018: GLOBOCAN estimates of incidence and mortality worldwide for 36 cancers in 185 countries. *CA: A Cancer Journal for Clinicians, 68*(6), 394-424.

Bremnes, T., Paasche, J. D., Mehlum, A., Sandberg, C., Bremnes, B., & Attramadal, H. (2000). Regulation and intracellular trafficking pathways of the endothelin receptors. *Journal of Biological Chemistry, 275*(23), 17596-17604.

Buckanovich, R. J., Facciabene, A., Kim, S., Benencia, F., Sasaroli, D., Balint, K., ... Coukos, G. (2008). Endothelin B receptor mediates the endothelial barrier to T cell homing to tumors and disables immune therapy. *Nature Medicine, 14*(1), 28-36.

Chen, C.-C., Chen, L.-L., Hsu, Y.-T., Liu, K.-J., Fan, C.-S., & Huang, T.-S. (2014). The endothelin-integrin axis is involved in macrophage-induced breast cancer cell chemotactic interactions with endothelial cells. *Journal of Biological Chemistry, 289*(14), 10029-10044.

Chester, A., & Yacoub, M. (2014). The role of endothelin-1 in pulmonary arterial hypertension. *Global Cardiology Science and Practice, 2014*, 62-78. doi:10.5339/gcsp.2014.29

Chikamatsu, K., Sakakura, K., Whiteside, T. L., & Furuya, N. (2007). Relationships between regulatory T cells and CD8+ effector populations in patients with squamous cell carcinoma of the head and neck. *Head and Neck: Journal for the Sciences and Specialties of the Head and Neck, 29*(2), 120-127.

Cianfrocca, R., Rosanò, L., Tocci, P., Sestito, R., Caprara, V., Di Castro, V., . . . Bagnato, A. (2017). Blocking endothelin-1-receptor/β-catenin circuit sensitizes to chemotherapy in colorectal cancer. *Cell Death and Differentiation, 24*(10), 1811-1820.

Clouthier, D. E., Hosoda, K., Richardson, J. A., Williams, S. C., Yanagisawa, H., Kuwaki, T., . . . Yanagisawa, M. (1998). Cranial and cardiac neural crest defects in endothelin-A receptor-deficient mice. Development, 125(5), 813-824

Condamine, T., Ramachandran, I., Youn, J.-I., & Gabrilovich, D. I. (2015). Regulation of tumor metastasis by myeloid-derived suppressor cells. *Annu Rev Med, 66*, 97-110.

Dandan, R., & Brunton, L. L. (2012). Endothelin A Receptor (ETAR). In S. Choi (Ed.), *Encyclopedia of Signaling Molecules* (pp. 545-551). New York, NY: Springer New York.

Davenport, A. P. (2002). International Union of Pharmacology. XXIX. Update on Endothelin Receptor Nomenclature. *Pharmacological Reviews, 54*(2), 219-226. doi:10.1124/pr.54.2.219

de Raaf, M. A., Beekhuijzen, M., Guignabert, C., Vonk Noordegraaf, A., & Bogaard, H. J. (2015). Endothelin-1 receptor antagonists in fetal development and pulmonary arterial hypertension. *Reproductive Toxicology, 56*, 45-51. doi:https://doi.org/10.1016/j.reprotox.2015.06.048

Del Bufalo, D., Di Castro, V., Biroccio, A., Varmi, M., Salani, D., Rosanò, L., . . . Bagnato, A. (2002). Endothelin-1 protects ovarian carcinoma cells against paclitaxel-induced apoptosis: requirement for Akt activation. *Molecular Pharmacology, 61*(3), 524-532.

Dexter, D. L., Kowalski, H. M., Blazar, B. A., Fligiel, Z., Vogel, R., & Heppner, G. H. (1978). Heterogeneity of tumor cells from a single mouse mammary tumor. *Cancer Research, 38*(10), 3174-3181.

DuPre, S. A., Redelman, D., & Hunter Jr, K. W. (2007). The mouse mammary carcinoma 4T1: characterization of the cellular landscape of primary tumours and metastatic tumour foci. *International Journal of Experimental Pathology, 88*(5), 351-360.

Emori, T., Hirata, Y., Imai, T., Ohta, K., Kanno, K., Eguchi, S., & Marumo, F. (1992). Cellular mechanism of thrombin on endothelin-1 biosynthesis and release in bovine endothelial cell. *Biochemical Pharmacology, 44*(12), 2409-2411.

Enevoldsen, F. C., Sahana, J., Wehland, M., Grimm, D., Infanger, M., & Krüger, M. (2020). Endothelin Receptor Antagonists: Status Quo and Future Perspectives for Targeted Therapy. *Journal of Clinical Medicine, 9*(3), 824. https://doi.org/10.3390/jcm9030824

Finn, O. J. (2008). Cancer immunology. *New England Journal of Medicine, 358*(25), 2704-2715.

Gabrilovich, D. I., & Nagaraj, S. (2009). Myeloid-derived suppressor cells as regulators of the immune system. *Nature Reviews Immunology, 9*(3), 162-174. doi:10.1038/nri2506

Galiè, N., Humbert, M., Vachiery, J.-L., Gibbs, S., Lang, I., Torbicki, A., . . . Beghetti, M. (2016). 2015 ESC/ERS guidelines for the diagnosis and treatment of pulmonary hypertension: the Joint Task Force for the Diagnosis and Treatment of Pulmonary Hypertension of the European Society of Cardiology (ESC) and the European Respiratory Society (ERS): endorsed by: Association for European Paediatric and Congenital Cardiology (AEPC), International Society for Heart and Lung Transplantation (ISHLT). *European Heart Journal, 37*(1), 67-119.

Galiè, N., Olschewski, H., Oudiz, R. J., Torres, F., Frost, A., Ghofrani, H. A., . . . Roecker, E. B. (2008). Ambrisentan in Pulmonary Arterial Hypertension, Randomized, Double-Blind, Placebo-Controlled, Multicenter, Efficacy Studies (ARIES) Group. Ambrisentan for the treatment of pulmonary arterial hypertension: results of the ambrisentan in pulmonary arterial hypertension, randomized, double-blind, placebo-controlled, multicenter, efficacy (ARIES) study 1 and 2. *Circulation, 117*(23), 3010-3019.

Gilman, A. G. (1984). G proteins and dual control of adenylate cyclase. *Cell, 36*(3), 577-579.

Guruli, G., Pflug, B. R., Pecher, S., Makarenkova, V., Shurin, M. R., & Nelson, J. B. (2004). Function and survival of dendritic cells depend on endothelin-1 and endothelin receptor autocrine loops. *Blood, 104*(7), 2107-2115.

Ha, N.-H., Nair, V. S., Reddy, D. N. S., Mudvari, P., Ohshiro, K., Ghanta, K. S., . . . Lipton, A. (2011). Lactoferrin–endothelin-1 axis contributes to the development and invasiveness of triple-negative breast cancer phenotypes. *Cancer Research, 71*(23), 7259-7269.

Hanahan, D., & Weinberg, R. A. (2011). Hallmarks of cancer: the next generation. *Cell, 144*(5), 646-674. doi:10.1016/j.cell.2011.02.013

Hou, H., Zhang, G., Wang, H., Gong, H., Wang, C., & Zhang, X. (2014). High matrix metalloproteinase-9 expression induces angiogenesis and basement membrane degradation in stroke-prone spontaneously hypertensive rats after cerebral infarction. *Neural Regeneration Research, 9*(11), 1154. doi:10.1097/moh.0b013e3282f97dbc

Houston, A., Bennett, M., O'Sullivan, G., Shanahan, F., & O'Connell, J. (2003). Fas ligand mediates immune privilege and not inflammation in human colon cancer, irrespective of TGF-β expression. *British Journal of Cancer, 89*(7), 1345-1351.

Hsieh, W.-T., Yeh, W.-L., Cheng, R.-Y., Lin, C., Tsai, C.-F., Huang, B.-R., . . . Lu, D.-Y. (2014). Exogenous endothelin-1 induces cell migration and matrix metalloproteinase expression in U251 human glioblastoma multiforme. *Journal of Neuro-Oncology, 118*(2), 257-269.

Huang, H. (2018). Matrix Metalloproteinase-9 (MMP-9) as a Cancer Biomarker and MMP-9 Biosensors: Recent Advances. *Sensors (Basel), 18*(10), 3249. doi:10.3390/s18103249

Hughes, C. C. (2008). Endothelial-stromal interactions in angiogenesis. *Current Opinion in Hematology, 15*(3), 204. doi:10.1097/moh.0b013e3282f97dbc

Hunter, K. W., Crawford, N. P. S., & Alsarraj, J. (2008). Mechanisms of metastasis. *Breast Cancer Research, 10*(1), S2. doi:10.1186/bcr1988

John, A., & Tuszynski, G. (2001). The role of matrix metalloproteinases in tumor angiogenesis and tumor metastasis. *Pathology Oncology Research, 7*(1), 14-23.

Kandalaft, L. E., Facciabene, A., Buckanovich, R. J., & Coukos, G. (2009). Endothelin B receptor, a new target in cancer immune therapy. *Clinical Cancer Research, 15*(14), 4521-4528.

Kandalaft, L. E., Motz, G. T., Duraiswamy, J., & Coukos, G. (2011). Tumor immune surveillance and ovarian cancer. *Cancer and Metastasis Reviews, 30*(1), 141-151.

Kang, Y., Siegel, P. M., Shu, W., Drobnjak, M., Kakonen, S. M., Cordón-Cardo, C., . . . Massagué, J. (2003). A multigenic program mediating breast cancer metastasis to bone. *Cancer Cell, 3*(6), 537-549.

Kappes, L., Amer, R. L., Sommerlatte, S., Bashir, G., Plattfaut, C., Gieseler, F., . . . Cabral-Marques, O. (2020). Ambrisentan, an endothelin receptor type A-selective antagonist, inhibits cancer cell migration, invasion, and metastasis. *Sci Rep, 10*(1), 15931. doi:10.1038/s41598-020-72960-1

Kessenbrock, K., Plaks, V., & Werb, Z. (2010). Matrix metalloproteinases: regulators of the tumor microenvironment. *Cell, 141*(1), 52-67.

Khimji, A.-k., & Rockey, D. C. (2010). Endothelin—biology and disease. *Cellular Signaling, 22*(11), 1615-1625.

Kim, M.-Y., Oskarsson, T., Acharyya, S., Nguyen, D. X., Zhang, X. H.-F., Norton, L., and Massagué, J. (2009). Tumor self-seeding by circulating cancer cells. *Cell, 139*(7), 1315-1326.

Kim, S.-J., Kim, J. S., Kim, S. W., Brantley, E., Yun, S. J., He, J., . . . Lehembre, F. (2011). Macitentan (ACT-064992), a tissue-targeting endothelin receptor antagonist, enhances therapeutic efficacy of paclitaxel by modulating survival pathways in orthotopic models of metastatic human ovarian cancer. *Neoplasia (New York, NY), 13*(2), 167. doi:10.1593/neo.10806

Kim, S.-J., Kim, J. S., Kim, S. W., Yun, S. J., He, J., Brantley, E., . . . Regenass, U. (2012). Antivascular therapy for multidrug-resistant ovarian tumors by macitentan, a dual endothelin receptor antagonist. *Translational Oncology, 5*(1), 39. doi:10.1593/tlo.11286

Kingman, M., Ruggiero, R., & Torres, F. (2009). Ambrisentan, an endothelin receptor type A-selective endothelin receptor antagonist, for the treatment of pulmonary arterial hypertension. *Expert Opinion on Pharmacotherapy, 10*(11), 1847-1858.

Kitadai, Y., Haruma, K., Sumii, K., Yamamoto, S., Ue, T., Yokozaki, H., . . . Fidler, I. J. (1998). Expression of interleukin-8 correlates with vascularity in human gastric carcinomas. *The American Journal of Pathology, 152*(1), 93. Retrieved from https://ajp.amjpathol.org/

Kohno, M., Horio, T., Yokokawa, K., Yasunari, K., Kurihara, N., & Takeda, T. (1994). Endothelin modulates the mitogenic effect of PDGF on glomerular mesangial cells. *Am J Physiol, 266*(6 Pt 2), F894-900. doi:10.1152/ajprenal.1994.266.6.F894

Kurihara, Y., Kurihara, H., Oda, H., Maemura, K., Nagai, R., Ishikawa, T., & Yazaki, Y. (1995). Aortic arch malformations and ventricular septal defect in mice deficient in endothelin-1. *The Journal of clinical investigation, 96*(1), 293-300.

Lee, Y.-M., Oh, M. H., Go, J.-H., Han, K., & Choi, S.-Y. (2020). Molecular subtypes of triple-negative breast cancer: understanding of subtype categories and clinical implication. *Genes and Genomics*, 1-7. doi: 10.1007/s13258-020-01014-7

Lefkowitz, R. J., & Shenoy, S. K. (2005). Transduction of receptor signals by ß-arrestins. *Science, 308*(5721), 512-517.

Lim, E., Modi, K. D., & Kim, J. (2009). In vivo bioluminescent imaging of mammary tumors using IVIS spectrum. *J Vis Exp* (26). doi:10.3791/1210

Liotta, L. A., & Kohn, E. C. (2001). The microenvironment of the tumour–host interface. *Nature, 411*(6835), 375-379.

Lu, X., & Kang, Y. (2009). Chemokine (CC motif) ligand 2 engages CCR2+ stromal cells of monocytic origin to promote breast cancer metastasis to lung and bone. *Journal of Biological Chemistry, 284*(42), 29087-29096.

Lu, Y., Cai, Z., Galson, D. L., Xiao, G., Liu, Y., George, D. E., . . . Zhang, J. (2006). Monocyte chemotactic protein-1 (MCP-1) acts as a paracrine and autocrine factor for prostate cancer growth and invasion. *The Prostate, 66*(12), 1311-1318.

Maffei, R., Bulgarelli, J., Fiorcari, S., Martinelli, S., Castelli, I., Valenti, V., . . . Potenza, L. (2014). Endothelin-1 promotes survival and chemoresistance in chronic lymphocytic leukemia B cells through ETA receptor. *PloS one, 9*(6). doi: 10.1371/journal.pone.0098818

Maguire, J. J., Kuc, R. E., Pell, V. R., Green, A., Brown, M., Kumar, S., . . . Davenport, A. P. (2012). Comparison of human ETA and ETB receptor signalling via G-protein and β-arrestin pathways. *Life Sciences, 91*(13-14), 544-549.

Marvel, D., & Gabrilovich, D. I. (2015). Myeloid-derived suppressor cells in the tumor microenvironment: expect the unexpected. *The Journal of Clinical Investigation, 125*(9), 3356-3364.

Masi, I., Caprara, V., Spadaro, F., Chellini, L., Sestito, R., Zancla, A., . . . Rosanò, L. (2021). Endothelin-1 drives invadopodia and interaction with mesothelial cells through ILK. *Cell Reports, 34*(9), 108800. doi:https://doi.org/10.1016/j.celrep.2021.108800

Medina, M. A., Oza, G., Sharma, A., Arriaga, L., Hernández Hernández, J. M., Rotello, V. M., & Ramirez, J. T. (2020). Triple-negative breast cancer: a review of conventional and advanced therapeutic strategies. *International Journal of Environmental Research and Public Health, 17*(6), 2078 doi:10.3390/ijerph17062078

Mehner, C., Hockla, A., Miller, E., Ran, S., Radisky, D. C., & Radisky, E. S. (2014). Tumor cell-produced matrix metalloproteinase 9 (MMP-9) drives malignant progression and metastasis of basal-like triple negative breast cancer. *Oncotarget, 5*(9), 2736. doi:10.18632/oncotarget.1932

Mestas, J., Burdick, M. D., Reckamp, K., Pantuck, A., Figlin, R. A., & Strieter, R. M. (2005). The role of CXCR2/CXCR2 ligand biological axis in renal cell carcinoma. *The Journal of Immunology, 175*(8), 5351-5357.

Miller, K., Moul, J., Gleave, M., Fizazi, K., Nelson, J., Morris, T., . . . Higano, C. (2013). Phase III, randomized, placebo-controlled study of once-daily oral zibotentan (ZD4054) in patients with non-metastatic castration-resistant prostate cancer. *Prostate Cancer and Prostatic Diseases, 16*(2), 187-192.

Miller, L., Kurtzman, S., Wang, Y., Anderson, K., Lindquist, R., & Kreutzer, D. (1998). Expression of interleukin-8 receptors on tumor cells and vascular endothelial cells in human breast cancer tissue. *Anticancer Research, 18*(1A), 77-81.

Minn, A. J., Gupta, G. P., Padua, D., Bos, P., Nguyen, D. X., Nuyten, D., . . . Ishwaran, H. (2007). Lung metastasis genes couple breast tumor size and metastatic spread. *Proceedings of the National Academy of Sciences, 104*(16), 6740-6745.

Minn, A. J., Gupta, G. P., Siegel, P. M., Bos, P. D., Shu, W., Giri, D. D., . . . Massagué, J. (2005). Genes that mediate breast cancer metastasis to lung. *Nature, 436*(7050), 518-524.

Morris, C., Rose, A., Curwen, J., Hughes, A., Wilson, D., & Webb, D. (2005). Specific inhibition of the endothelin A receptor with ZD4054: clinical and pre-clinical evidence. *British Journal of Cancer, 92*(12), 2148-2152.

Müller, A., Homey, B., Soto, H., Ge, N., Catron, D., Buchanan, M. E., . . . Wagner, S. N. (2001). Involvement of chemokine receptors in breast cancer metastasis. *Nature, 410*(6824), 50-56.

Murphy, G. (2005). Atrasentan for metastatic hormone refractory prostate cancer. *Issues in Emerging Health Technologies* (77), 1-4. doi:10.1016/s1540-0352(11)70025-7

Nagaraj, S., & Gabrilovich, D. I. (2007). Myeloid-derived suppressor cells. *Immune-Mediated Diseases*, 213-223. doi:10.1007/978-0-387-72005-0_22

Nelson, J., Bagnato, A., Battistini, B., & Nisen, P. (2003). The endothelin axis: emerging role in cancer. *Nature Reviews Cancer, 3*(2), 110-116.

Nelson, J. B., Hedican, S. P., George, D. J., Reddi, A. H., Piantadosi, S., Eisenberger, M. A., & Simons, J. W. (1995). Identification of endothelin–1 in the pathophysiology of metastatic adenocarcinoma of the prostate. *Nature Medicine, 1*(9), 944-949.

Nelson, J. B., Udan, M. S., Guruli, G., & Pflug, B. R. (2005). Endothelin-1 inhibits apoptosis in prostate cancer. *Neoplasia (New York, NY), 7*(7), 631. doi:10.1593/neo.04787

Newman, J. H., Kar, S., & Kirkpatrick, P. (2007). Ambrisentan: Nature Publishing Group.

Nie, S., Zhou, J., Bai, F., Jiang, B., Chen, J., & Zhou, J. (2014). Role of endothelin A receptor in colon cancer metastasis: in vitro and in vivo evidence. *Molecular Carcinogenesis, 53*(S1), E85-E91.

Ohlstein, E. H., Elliott, J. D., Feuerstein, G. Z., & Ruffolo, R. R. (1996). Endothelin receptors: receptor classification, novel receptor antagonists, and potential therapeutic targets. *Medicinal Research Reviews, 16*(4), 365-390. doi:10.1002/(sici)1098-1128(199607)16:4%3C365::aid-med4%3E3.0.co;2-v

Ortega, N., Behonick, D. J., Colnot, C., Cooper, D. N., & Werb, Z. (2005). Galectin-3 is a downstream regulator of matrix metalloproteinase-9 function during endochondral bone formation. *Molecular Biology of The Cell, 16*(6), 3028-3039.

Ostrand-Rosenberg, S., & Sinha, P. (2009). Myeloid-derived suppressor cells: linking inflammation and cancer. *The Journal of Immunology, 182*(8), 4499-4506.

Ouzounova, M., Lee, E., Piranlioglu, R., El Andaloussi, A., Kolhe, R., Demirci, M. F., . . . Hassan, K. A. (2017). Monocytic and granulocytic myeloid derived suppressor cells differentially regulate spatiotemporal tumour plasticity during metastatic cascade. *Nature Communications, 8*(1), 1-13.

Owen, J. D., Strieter, R., Burdick, M., Haghnegahdar, H., Nanney, L., Shattuck-Brandt, R., & Richmond, A. (1997). Enhanced tumor-forming capacity for immortalized melanocytes expressing melanoma growth stimulatory activity/growth-regulated cytokine β and γ proteins. *International Journal of Cancer, 73*(1), 94-103.

Pla, P., & Larue, L. (2003). Involvement of endothelin receptors in normal and pathological development of neural crest cells. *International Journal of Developmental Biology, 47*(5), 315-325.

Pollock, D. M., Keith, T. L., & Highsmith, R. F. (1995). Endothelin receptors and calcium signaling 1. *The FASEB Journal, 9*(12), 1196-1204.

Polyak, K., & Weinberg, R. A. (2009). Transitions between epithelial and mesenchymal states: acquisition of malignant and stem cell traits. *Nature Reviews Cancer, 9*(4), 265-273.

Pulaski, B. A., & Ostrand-Rosenberg, S. (2000). Mouse 4T1 breast tumor model. *Current Protocols in Immunology,39*(1).doi:10.1002/0471142735.im2002s39

Qian, B.-Z., Li, J., Zhang, H., Kitamura, T., Zhang, J., Campion, L. R., . . . Pollard, J. W. (2011). CCL2 recruits inflammatory monocytes to facilitate breast-tumour metastasis. *Nature, 475*(7355), 222-225.

Radisky, E. S., & Radisky, D. C. (2007). Stromal induction of breast cancer: inflammation and invasion. *Reviews in Endocrine and Metabolic Disorders, 8*(3), 279-287.

Ribatti, D. (2017). The chick embryo chorioallantoic membrane (CAM) assay. *Reprod Toxicol, 70*, 97-101. doi: 10.1016/j.reprotox.2016.11.004

Richards, B. L., Eisma, R. J., Spiro, J. D., Lindquist, R. L., & Kreutzer, D. L. (1997). Coexpression of interleukin-8 receptors in head and neck squamous cell carcinoma. *The American Journal of Surgery, 174*(5), 507-512.

Robinson, S. C., Scott, K. A., Wilson, J. L., Thompson, R. G., Proudfoot, A. E., & Balkwill, F. R. (2003). A chemokine receptor antagonist inhibits experimental breast tumor growth. *Cancer Research, 63*(23), 8360-8365.

Rosanò, L., & Bagnato, A. (2016). Endothelin therapeutics in cancer: Where are we? *American Journal of Physiology-Regulatory, Integrative and Comparative Physiology, 310*(6), R469-R475.

Rosanò, L., & Bagnato, A. (2019). Chapter Four - New insights into the regulation of the actin cytoskeleton dynamics by GPCR/β-arrestin in cancer invasion and metastasis. In L. Galluzzi (Ed.), *International Review of Cell and Molecular Biology* (Vol. 346, pp. 129-155): Academic Press.

Rosanò, L., Cianfrocca, R., Tocci, P., Spinella, F., Di Castro, V., Caprara, V., . . . Bagnato, A. (2014). Endothelin A receptor/β-arrestin signaling to the Wnt pathway renders ovarian cancer cells resistant to chemotherapy. *Cancer Research, 74*(24), 7453-7464.

Rosanò, L., Spinella, F., & Bagnato, A. (2013). Endothelin 1 in cancer: biological implications and therapeutic opportunities. *Nature Reviews Cancer, 13*(9), 637-651.

Rosanò, L., Spinella, F., Di Castro, V., Dedhar, S., Nicotra, M. R., Natali, P. G., & Bagnato, A. (2006). Integrin-linked kinase functions as a downstream mediator of endothelin-1 to promote invasive behavior in ovarian carcinoma. *Molecular Cancer Therapeutics, 5*(4), 833-842.

Rosano, L., Spinella, F., Salani, D., Di Castro, V., Venuti, A., Nicotra, M. R., . . . Bagnato, A. (2003). Therapeutic targeting of the endothelin a receptor in human ovarian carcinoma. *Cancer Research, 63*(10), 2447-2453.

Rosanò, L., Varmi, M., Salani, D., Di Castro, V., Spinella, F., Natali, P. G., & Bagnato, A. (2001). Endothelin-1 induces tumor proteinase activation and invasiveness of ovarian carcinoma cells. *Cancer Research, 61*(22), 8340-8346.

Roux, S., & Rubin, L. J. (2002). Bosentan: a dual endothelin receptor antagonist. *Expert Opinion on Investigational Drugs, 11*(7), 991-1002.

Russell, F. D., Skepper, J. N., & Davenport, A. P. (1998). Human endothelial cell storage granules: a novel intracellular site for isoforms of the endothelin-converting enzyme. *Circulation Research, 83*(3), 314-321.

Said, N., Smith, S., Sanchez-Carbayo, M., & Theodorescu, D. (2011). Tumor endothelin-1 enhances metastatic colonization of the lung in mouse xenograft models of bladder cancer. *The Journal of Clinical Investigation, 121*(1), 132-147.

Salani, D., Di Castro, V., Nicotra, M. R., Rosanò, L., Tecce, R., Venuti, A., . . . Bagnato, A. (2000). Role of endothelin-1 in neovascularization of ovarian carcinoma. *The American Journal of Pathology, 157*(5), 1537-1547.

Salani, D., Taraboletti, G., Rosanò, L., Di Castro, V., Borsotti, P., Giavazzi, R., & Bagnato, A. (2000). Endothelin-1 induces an angiogenic phenotype in cultured endothelial cells and stimulates neovascularization in vivo. *The American Journal of Pathology, 157*(5), 1703-1711.

Sasaki, Y., Hori, S., Oda, K., Okada, T., & Takimoto, M. (1998). Both ETA and ETB receptors are involved in mitogen-activated protein kinase activation and DNA synthesis of astrocytes: study using ETB receptor-deficient rats (aganglionosis rats). *European Journal of Neuroscience, 10*(9), 2984-2993.

Sawant, K. V., Poluri, K. M., Dutta, A. K., Sepuru, K. M., Troshkina, A., Garofalo, R. P., & Rajarathnam, K. (2016). Chemokine CXCL1 mediated neutrophil recruitment: Role of glycosaminoglycan interactions. *Scientific Reports, 6*(1), 33123. doi:10.1038/srep33123

Schmielau, J., & Finn, O. J. (2001). Activated granulocytes and granulocyte-derived hydrogen peroxide are the underlying mechanism of suppression of t-cell function in advanced cancer patients. *Cancer Research, 61*(12), 4756-4760.

Semprucci, E., Tocci, P., Cianfrocca, R., Sestito, R., Caprara, V., Veglione, M., . . . Bagnato, A. (2016). Endothelin A receptor drives invadopodia function and cell motility through the β-arrestin/PDZ-RhoGEF pathway in ovarian carcinoma. *Oncogene, 35*(26), 3432-3442.

Sestito, R., Cianfrocca, R., Rosanò, L., Tocci, P., Di Castro, V., Caprara, V., & Bagnato, A. (2016). Macitentan blocks endothelin-1 receptor activation required for chemoresistant ovarian cancer cell plasticity and metastasis. *Life Sciences, 159*, 43-48.

Shukla, A. K., Xiao, K., & Lefkowitz, R. J. (2011). Emerging paradigms of β-arrestin-dependent seven transmembrane receptor signaling. *Trends in Biochemical Sciences, 36*(9), 457-469.

Sidharta, P. N., van Giersbergen, P. L., & Dingemanse, J. (2013). Safety, tolerability, pharmacokinetics, and pharmacodynamics of macitentan, an endothelin receptor antagonist, in an ascending multiple-dose study in healthy subjects. *The Journal of Clinical Pharmacology, 53*(11), 1131-1138.

Sidharta, P. N., van Giersbergen, P. L., Halabi, A., & Dingemanse, J. (2011). Macitentan: entry-into-humans study with a new endothelin receptor antagonist. *European Journal of Clinical Pharmacology, 67*(10), 977. doi: 10.1007/s00228-011-1043-2

Sinha, P., Clements, V. K., Bunt, S. K., Albelda, S. M., & Ostrand-Rosenberg, S. (2007). Cross-talk between myeloid-derived suppressor cells and macrophages subverts tumor immunity toward a type 2 response. *The Journal of Immunology, 179*(2), 977-983.

Smollich, M., Götte, M., Kersting, C., Fischgräbe, J., Kiesel, L., & Wülfing, P. (2008). Selective ET AR antagonist atrasentan inhibits hypoxia-induced breast cancer cell invasion. *Breast Cancer Research and Treatment, 108*(2), 175-182.

Soria, G., Yaal-Hahoshen, N., Azenshtein, E., Shina, S., Leider-Trejo, L., Ryvo, L., . . . Meshel, T. (2008). Concomitant expression of the chemokines RANTES and MCP-1 in human breast cancer: a basis for tumor-promoting interactions. *Cytokine, 44*(1), 191-200.

Spinella, F., Garrafa, E., Di Castro, V., Rosanò, L., Nicotra, M. R., Caruso, A., . . . Bagnato, A. (2009). Endothelin-1 stimulates lymphatic endothelial cells and lymphatic vessels to grow and invade. *Cancer Research, 69*(6), 2669-2676.

Stamenkovic, I. (2003). Extracellular matrix remodelling: the role of matrix metalloproteinases. *The Journal of Pathology: A Journal of the Pathological Society of Great Britain and Ireland, 200*(4), 448-464.

Stormes, K. A., Lemken, C. A., Lepre, J. V., Marinucci, M. N., & Kurt, R. A. (2005). Inhibition of metastasis by inhibition of tumor-derived CCL5. *Breast Cancer Research and Treatment, 89*(2), 209-212.

Teicher, B. A. (2007). Transforming growth factor-β and the immune response to malignant disease. *Clinical Cancer Research, 13*(21), 6247-6251.

Titus, B., Frierson, H. F., Conaway, M., Ching, K., Guise, T., Chirgwin, J., . . . Theodorescu, D. (2005). Endothelin axis is a target of the lung metastasis suppressor gene RhoGDI2. *Cancer Research, 65*(16), 7320-7327.

Tocci, P., Caprara, V., Cianfrocca, R., Sestito, R., Di Castro, V., Bagnato, A., & Rosanò, L. (2016). Endothelin-1/endothelin A receptor axis activates RhoA GTPase in epithelial ovarian cancer. *Life Sciences, 159*, 49-54.

Tuteja, N. (2009). Signaling through G protein coupled receptors. *Plant Signaling and Behavior, 4*(10), 942-947. doi:10.4161/psb.4.10.9530

Ueno, T., Toi, M., Saji, H., Muta, M., Bando, H., Kuroi, K., . . . Matsushima, K. (2000). Significance of macrophage chemoattractant protein-1 in macrophage recruitment, angiogenesis, and survival in human breast cancer. *Clinical Cancer Research, 6*(8), 3282-3289.

Velasco-Velázquez, M., Jiao, X., De La Fuente, M., Pestell, T. G., Ertel, A., Lisanti, M. P., & Pestell, R. G. (2012). CCR5 antagonist blocks metastasis of basal breast cancer cells. *Cancer Research, 72*(15), 3839-3850.

Wang, J., Gareri, C., & Rockman, H. A. (2018). G-Proteinand#x2013;Coupled Receptors in Heart Disease. *Circulation Research, 123*(6), 716-735. doi:10.1161/CIRCRESAHA.118.311403

Wendel, C., Hemping-Bovenkerk, A., Krasnyanska, J., Mees, S. T., Kochetkova, M., Stoeppeler, S., & Haier, J. (2012). CXCR4/CXCL12 participate in extravasation of metastasizing breast cancer cells within the liver in a rat model. *PloS one, 7*(1), e30046. doi: 10.1371/journal.pone.0030046

Whipple, C., & Korc, M. (2008). Targeting angiogenesis in pancreatic cancer: rationale and pitfalls. *Langenbeck's Archives of Surgery, 393*(6), 901-910.

Whipple, C. A., & Korc, M. (2010). Angiogenesis Signaling Pathways as Targets in Cancer Therapy *Handbook of Cell Signaling* (pp. 2895-2905): Elsevier.

Witteveen, P. O., van der Mijn, K. J., Los, M., Kronemeijer, R. H., Groenewegen, G., & Voest, E. E. (2010). Phase 1/2 study of atrasentan combined with pegylated liposomal doxorubicin in platinum-resistant recurrent ovarian cancer. *Neoplasia (New York, NY), 12*(11), 941. doi:10.1593/neo.10582

Wolf, M. J., Hoos, A., Bauer, J., Boettcher, S., Knust, M., Weber, A., . . . Stürzl, M. (2012). Endothelial CCR2 signaling induced by colon carcinoma cells enables extravasation via the JAK2-Stat5 and p38MAPK pathway. *Cancer Cell, 22*(1), 91-105.

Woo, E. Y., Chu, C. S., Goletz, T. J., Schlienger, K., Yeh, H., Coukos, G., . . . June, C. H. (2001). Regulatory CD4+ CD25+ T cells in tumors from patients with early-stage non-small cell lung cancer and late-stage ovarian cancer. *Cancer Research, 61*(12), 4766-4772.

Wu, M. H., Huang, C.-Y., Lin, J., Wang, S.-W., Peng, C.-Y., Cheng, H.-C., & Tang, C.-H. (2014). Endothelin-1 promotes vascular endothelial growth factor-dependent angiogenesis in human chondrosarcoma cells. *Oncogene, 33*(13), 1725-1735.

Wu, M. H., Lo, J. F., Kuo, C. H., Lin, J. A., Lin, Y. M., Chen, L. M., . . . Tang, C. H. (2012). Endothelin-1 promotes MMP-13 production and migration in human chondrosarcoma cells through FAK/PI3K/Akt/mTOR pathways. *Journal of Cellular Physiology, 227*(8), 3016-3026.

Wülfing, P., Götte, M., Sonntag, B., Kersting, C., Schmidt, H., Wülfing, C., . . . Kiesel, L. (2005). Overexpression of Endothelin-A-receptor in breast cancer: regulation by estradiol and cobalt-chloride induced hypoxia. *International Journal of Oncology, 26*(4), 951-960.

Xie, H.-Y., Shao, Z.-M., & Li, D.-Q. (2017). Tumor microenvironment: driving forces and potential therapeutic targets for breast cancer metastasis. *Chinese Journal of Cancer, 36*(1), 1-10.

Xu, D., Emoto, N., Giaid, A., Slaughter, C., Kaw, S., DeWit, D., & Yanagisawa, M. (1994). ECE-1: a membrane-bound metalloprotease that catalyzes the proteolytic activation of big endothelin-1. *Cell, 78*(3), 473-485.

Yanagisawa, M., Kurihara, H., Kimura, S., Tomobe, Y., Kobayashi, M., Mitsui, Y., . . . Masaki, T. (1988). A novel potent vasoconstrictor peptide produced by vascular endothelial cells. *Nature, 332*(6163), 411-415. doi:10.1038/332411a0

Yoshidome, H., Kohno, H., Shida, T., Kimura, F., Shimizu, H., Ohtsuka, M., . . . Miyazaki, M. (2009). Significance of monocyte chemoattractant protein-1 in angiogenesis and survival in colorectal liver metastases. *International Journal of Oncology, 34*(4), 923-930.

Yousef, E. M., Tahir, M. R., St-Pierre, Y., & Gaboury, L. A. (2014). MMP-9 expression varies according to molecular subtypes of breast cancer. *BMC Cancer, 14*(1), 1-12.

Zetter, B. R. (1998). Angiogenesis and tumor metastasis. *Annu Rev Med, 49*, 407-424. doi:10.1146/annurev.med.49.1.407

Zhao, L., Lim, S. Y., Gordon-Weeks, A. N., Tapmeier, T. T., Im, J. H., Cao, Y., . . . Muschel, R. J. (2013). Recruitment of a myeloid cell subset (CD11b/Gr1mid) via CCL2/CCR2 promotes the development of colorectal cancer liver metastasis. *Hepatology, 57*(2), 829-839.

Zijlmans, H. J., Fleuren, G. J., Baelde, H. J., Eilers, P. H., Kenter, G. G., & Gorter, A. (2006). The absence of CCL2 expression in cervical carcinoma is associated with increased survival and loss of heterozygosity at 17q11. 2. *The Journal of Pathology: A Journal of the Pathological Society of Great Britain and Ireland, 208*(4), 507-517.

List of Publications

Kappes, L., R. L. Amer, S. Sommerlatte, G. Bashir, C. Plattfaut, F. Gieseler, T. Gemoll, H. Busch, A. Al-Tahrawi, A. Al-Sbiei, S.M. Haneefa, K. Arafat, L.F. Schimke, N. El Khawanky, A. Mueller, H. Heidecke, S. Attoub, M.J. Fernandez-Cabezudo, G. Riemekasten, B.K. al-Ramadi, & O. Cabral-Marques. (2020). Ambrisentan, an endothelin receptor type A-selective antagonist, inhibits cancer cell migration, invasion, and metastasis. *Scientific Reports* 28;10(1):15931. doi: 10.1038/s41598-020-72960-1